Stem Cell Reports
Article

ISSCR

OPEN ACCESS

Induced Fetal Human Muscle Stem Cells with High Therapeutic Potential in a Mouse Muscular Dystrophy Model

Mingming Zhao,[1,6,*] Atsutoshi Tazumi,[1,2,6] Satoru Takayama,[1,2,6] Nana Takenaka-Ninagawa,[1] Minas Nalbandian,[1] Miki Nagai,[1] Yumi Nakamura,[1] Masanori Nakasa,[1] Akira Watanabe,[3] Makoto Ikeya,[1] Akitsu Hotta,[1] Yuta Ito,[4] Takahiko Sato,[5] and Hidetoshi Sakurai[1,*]

[1]Department of Clinical Application, Center for iPS Cell Research and Application (CiRA), Kyoto University, 53 Shogoin-Kawahara-cho, Sakyo-ku, Kyoto 606-8507, Japan
[2]Asahi Kasei Co., Ltd., 1-105 Jinbo-cho, Kanda, Chiyoda-ku, Tokyo, Japan
[3]Department of Life Science Frontiers, Center for iPS Cell Research and Application (CiRA), Kyoto University, 53 Shogoin-Kawahara-cho, Sakyo-ku, Kyoto 606-8507, Japan
[4]Faculty of Rehabilitation Science, Nagoya Gakuin University, 1350 Kamishinano-cho, Seto City, Aichi 480-1298, Japan
[5]Department of Anatomy, Fujita Health University, 1-98 Dengakugakubo, Kutsukake-cho, Toyoake, Aichi 470-1192, Japan
[6]Co-first author
*Correspondence: zhaoming@cira.kyoto-u.ac.jp (M.Z.), hsakurai@cira.kyoto-u.ac.jp (H.S.)
https://doi.org/10.1016/j.stemcr.2020.06.004

SUMMARY

Duchenne muscular dystrophy (DMD) is a progressive and fatal muscle-wasting disease caused by DYSTROPHIN deficiency. Cell therapy using muscle stem cells (MuSCs) is a potential cure. Here, we report a differentiation method to generate fetal MuSCs from human induced pluripotent stem cells (iPSCs) by monitoring MYF5 expression. Gene expression profiling indicated that MYF5-positive cells in the late stage of differentiation have fetal MuSC characteristics, while MYF5-positive cells in the early stage of differentiation have early myogenic progenitor characteristics. Moreover, late-stage MYF5-positive cells demonstrated good muscle regeneration potential and produced DYSTROPHIN *in vivo* after transplantation into DMD model mice, resulting in muscle function recovery. The engrafted cells also generated PAX7-positive MuSC-like cells under the basal lamina of DYSTROPHIN-positive fibers. These findings suggest that MYF5-positive fetal MuSCs induced in the late stage of iPSC differentiation have cell therapy potential for DMD.

INTRODUCTION

Duchenne muscular dystrophy (DMD) is one of the most common types of muscular dystrophy with onset in childhood. DMD patients show severe and progressive muscle atrophy and weakness, eventually resulting in a loss of walking ability and respiratory deficiency (Fairclough et al., 2013). The causative gene, *DMD*, encodes the DYSTROPHIN protein, which binds F-actin and sarcolemma in the cytoskeleton (Hoffman et al., 1987). The majority of DMD patients show deletions or mutations in *DMD*, resulting in a loss of DYSTROPHIN protein expression (White et al., 2002). Since the restoration of DYSTROPHIN expression has been thought to be a definitive treatment for DMD, several therapeutic approaches have been investigated, such as mutation-specific drug exon skipping (Kinali et al., 2009; Muntoni and Wood, 2011), gene therapy (Fairclough et al., 2013; Nowak and Davies, 2004), and cell therapy (Tremblay, 2006).

Among these approaches, cell therapy is expected to be the most promising because adult muscle stem cells (MuSCs), or satellite cells, possess robust regeneration potential for injured muscle. Previous studies have shown that transplanted adult MuSCs into model mice of muscular dystrophy fuse to the host muscle fibers and recover muscular function, suggesting regenerative properties (Cerletti et al., 2008; Marg et al., 2014; Montarras et al., 2005; Sacco et al., 2008; Tanaka et al., 2009; Xu et al., 2015). However, the expansion of adult MuSCs with stemness is difficult (Gilbert et al., 2010; Montarras et al., 2005; Negroni et al., 2009; Sacco et al., 2008). On the other hand, fetal MuSCs can be expanded without compromising stemness and have higher engraftment efficiency than adult MuSCs (Tierney et al., 2016).

Human induced pluripotent stem cells (hiPSCs) are an attractive cell source for various cell therapies due to their proliferation and differentiation potential (Takahashi et al., 2007). In the field of muscular dystrophy, several types of skeletal muscle progenitors with regeneration potential for injured muscle have been differentiated from hiPSCs via the virus-mediated overexpression of myogenic transcription factors (Albini et al., 2013; Darabi et al., 2012; Rao et al., 2012, 2018; Shoji et al., 2015). Darabi et al. (2012) reported that their muscle progenitors, iPAX7, exerted particularly high regenerative potential when grafted into DMD model mice. However, the safety of these cells, especially tumorigenicity, must be carefully evaluated before clinical trials since the hiPSCs were modified with a doxycycline-inducible lentiviral vector encoding PAX7. Transgene-free protocols that recapitulate the development of muscle lineage beginning with iPSCs by the stepwise addition of small chemicals and growth factors have also been reported (Barberi et al., 2007; Caron et al., 2016; Chal et al., 2015, 2016; Shelton et al., 2014; Yu

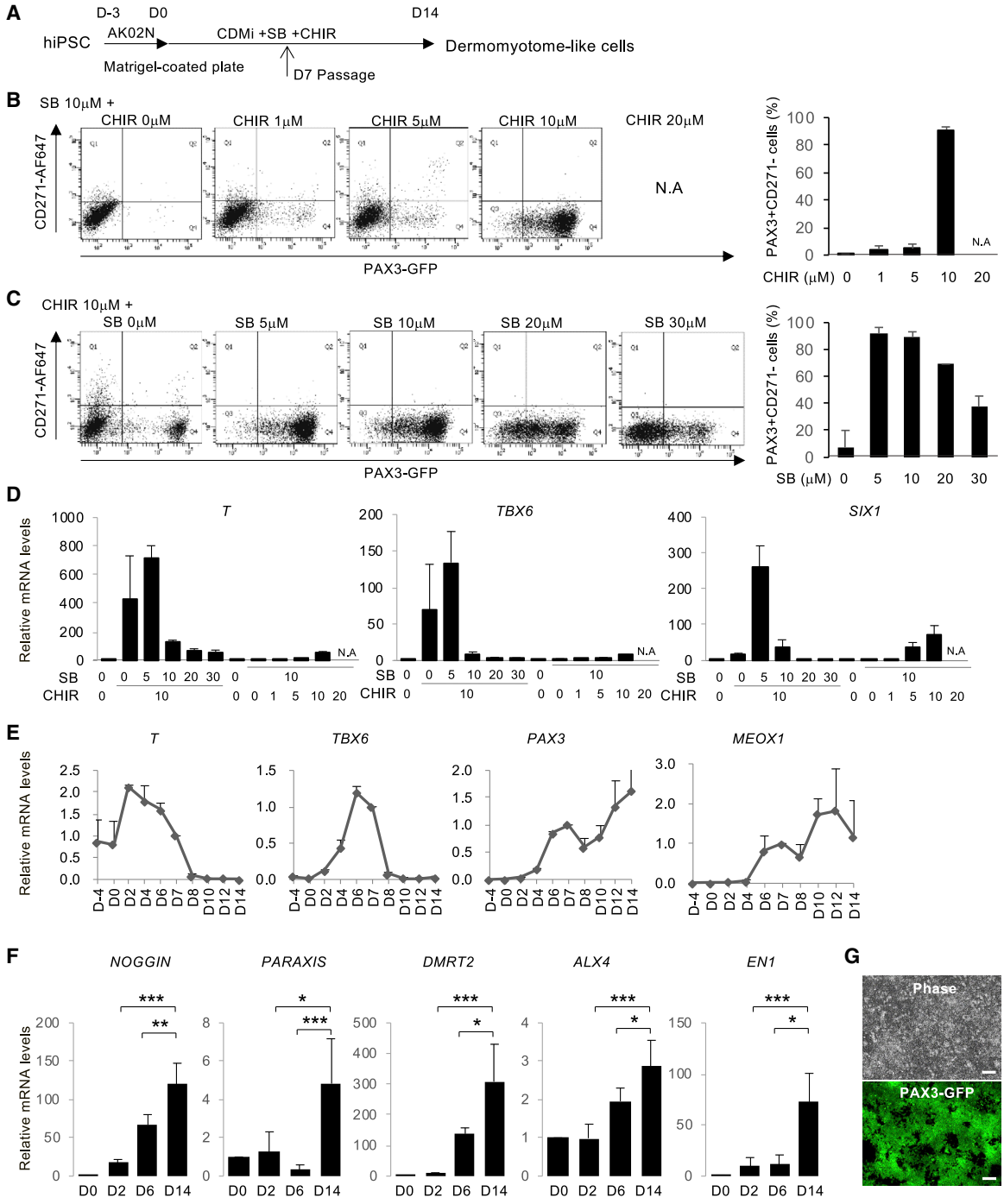

Figure 1. Screening with PAX3-GFP reporter line to optimize dermomyotome lineage induction from hiPSCs

(A) The step-wise differentiation protocol for hiPSC-derived dermomyotome. hiPSCs were plated in Matrigel-coated plates cultured in Stemfit (AK02N) for 3 days. The medium was changed to CDMi supplemented with SB431542 (SB) and CHIR99021 (CHIR) and then cultured for 14 days. Cells were passaged on day 7 and as single cells thereafter on a Matrigel-coated plate.

(B) hiPSCs were treated with SB (10 μM) and CHIR (0 , 1, 5, 10, or 20 μM). The histogram shows the ratio of PAX3+CD271− cells in the whole cell population. CHIR increased the PAX3+CD271− cell population dose dependently. 10 μM CHIR and 10 μM SB induced 90% PAX3+CD271− cells. CHIR (20 μM) was toxic to hiPSCs and caused cell death (data not shown). Data of three independent experiments are shown as means ± SD. N.A., not available.

(legend continued on next page)

et al., 2007). Although these protocols have lower health risks compared with iPAX7, the muscular regeneration is weaker (Kim et al., 2017).

Here, we report a novel transgene-free differentiation protocol from hiPSCs into fetal MuSCs with higher regeneration potential than iPAX7. Using a GFP reporter line with the dermomyotome marker PAX3 knocked in, we found that relatively long and strong activation of the WNT/β-CATENIN signaling pathway leads to the efficient induction of PAX3-GFP-positive dermomyotome-like cells. To visualize the myogenic lineage commitment, we generated a tdTomato reporter line with the myogenic progenitor marker MYF5 knocked in and examined the differentiation condition of muscle lineage cells from dermomyotome-like cells. Interestingly, the characteristics of MYF5-tdTomato-positive cells significantly changed with the duration of the differentiation steps. MYF5-tdTomato-positive cells at the early stage of differentiation resembled early myogenic progenitors, whereas those at the later stage resembled fetal MuSCs and expressed *PAX7*. The late-stage MYF5-tdTomato-positive cells recovered DYSTROPHIN and were maintained as PAX7-expressing satellite-like cells when grafted into DMD-null/NSG mice. Moreover, the limbs in which the cells were engrafted showed significantly higher contraction compared with control limbs. Thus, hiPSC-derived late-stage MYF5-positive cells, such as MuSCs, show good regenerative properties and should be investigated for transplantation therapy in the future.

RESULTS

Optimized Induction Method of Dermomyotome-like Lineage from hiPSCs with PAX3-GFP Reporter Line

To screen for the optimal condition that induces dermomyotome-like lineage from hiPSCs, we established the PAX3-GFP knockin 201B7 hiPSC line (Takahashi et al., 2007) using the BAC construct-based recombination method (Figure S1A). We confirmed the recombination by quantitative real-time PCR (Figure S1B) and selected clone no. 142 as a heterozygous targeted clone. After conventional embryoid body formation, GFP-positive cells were observed and isolated by flow cytometry (Figure S1C and S1D). *PAX3* expression in the GFP-positive population was confirmed by RT-PCR (Figure S1E) and immunostaining (Figure S1F). Then we optimized the dermomyotome induction condition by monitoring PAX3-GFP expression. Using the neural crest marker CD271, we excluded neural crest cells from the dermomyotome lineage (Figures S2A–S2C), since PAX3 is also known as a marker of neural crest lineage (Goulding et al., 1991). Previously, the inhibition of transforming growth factor β signaling by SB431542 (SB) was reported to promote the myogenic differentiation of human pluripotent stem cells (Mahmood et al., 2010), and the activation of WNT signaling by the inhibition of glycogen synthase kinase-3β(GSK-3β) was also reported to promote myogenic differentiation through dermomyotome formation (Borchin et al., 2013; Choi et al., 2016; Xu et al., 2015). Therefore, we attempted to induce dermomyotome lineage by combining SB and a GSK-3β inhibitor, CHIR99021 (CHIR) (Figure 1A). First, we optimized the concentration of CHIR in chemically defined medium (CDMi) supplemented with 10 μM SB (Figure 1B). Dermomyotome lineage was assessed as the PAX3-GFP-positive and CD271-negative population by fluorescence-activated cell sorting. PAX3+CD271− dermomyotome lineage was robustly induced when 10 μM CHIR was added for 14 days (Figure 1B). Accordingly, we optimized the SB concentration supplemented with 10 μM CHIR. The addition of 5 or 10 μM SB robustly promoted the PAX3+CD271− population in more than 90% of differentiated cells (Figure 1C). We confirmed step-wise differentiation by analyzing the expression of an early mesoderm marker, *T* (Hashimoto et al., 1987), a paraxial mesoderm marker, *TBX6* (Chapman et al., 1996), and a dermomyotome marker, *SIX1* (Nord et al., 2013) (Figure 1D). The induction

(C) hiPSCs were treated with CHIR (10 μM) and SB (0, 5, 10, 20, or 30 μM). The histogram shows the ratio of PAX3+CD271− cells in the whole cell population. 10 μM CHIR and 5 μM SB induced 95% PAX3+CD271− cells. Data of three independent experiments are shown as means ± SD.

(D) mRNA expressions of *T* (day 6), *TBX6* (day 6), and *SIX1* (day 14) induced by CHIR and SB. Cells were treated with CHIR and SB at the indicated concentrations (μM). Data of three independent experiments are shown as means ± SD.

(E) Time course of the mRNA expression of *BRACHYURY (T)*, *TBX6*, *PAX3*, and *MEOX1* in hiPSCs treated with 10 μM CHIR and 5 μM SB. The results are shown relative to values of human teratoma cells. Data of three independent experiments are shown as means ± SD. Primitive streak marker (*T*), paraxial mesoderm marker (*TBX6*), and dermomyotome marker (*SIX1*) were strongly upregulated on days 2, 6, and 14, respectively.

(F) Time course of the mRNA expression of the dermomyotome markers *NOGGIN*, *PARAXIS*, *DMRT2*, *ALX4*, and *EN1* on days 0, 2, 6, and 14 of the differentiation. Dermomyotome marker genes time dependently increased in this step-wise protocol. Data of three independent experiments are shown as means ± SD. *$p < 0.05$, **$p < 0.01$, ***$p < 0.001$.

(G) Phase and fluorescence images of PAX3-GFP reporter cells differentiated using the step-wise protocol in (A). Almost all of the differentiated cells were GFP+ cells. Scale bars, 100 μm.

of *T* and *TBX6* was promoted by the addition of 10 μM CHIR and 0 or 5 μM SB (Figure 1D), suggesting that a high CHIR dose dominantly promotes early mesoderm and paraxial mesoderm differentiation. On the other hand, the induction of *SIX1* was specifically promoted by the addition of 10 μM CHIR and 5 μM SB (Figure 1D), suggesting that SB treatment is necessary to promote dermomyotome specification from paraxial mesoderm. We defined the addition of 10 μM CHIR and 5 μM SB in CDMi as the dermomyotome induction condition. Time course expression profiling of the marker genes was performed to confirm the step-wise differentiation toward dermomyotome (Figure 1E). The expression level of *T* first reached a peak at day 2, and the expression level of *TBX6* reached a peak at day 6 (Figure 1E). The expression level of two dermomyotome markers, *PAX3* and *MEOX1*, gradually increased during the 14 days of differentiation (Figure 1E). *NOGGIN*, *PARAXIS*, *DMRT2*, *ALX4*, and *EN1* were used as dermomyotome markers (Nakajima et al., 2018; Sato et al., 2010), CDMi supplemented with 10 μM CHIR and 5 μM SB also gradually increased the expression of these dermomyotome markers during the 14-day differentiation (Figure 1F). These results suggest that the dermomyotome induction condition mimics the developmental steps toward dermomyotome. Morphologically, PAX3-GFP-positive cells represented an epithelial cell-like structure at day 14 (Figure 1G). Several recent studies, recapitulating the development of muscle lineage, differentiated hiPSCs by modulating signaling pathways to induce a paraxial mesoderm fate and then a dermomyotome fate (Chal et al., 2015; Hicks et al., 2018; Shelton et al., 2014). Method S (Shelton et al., 2014) and method C (Chal et al., 2015) were selected to be compared with our protocol, method Z (Figure 2A). Method Z significantly increased the PAX3+CD271− population at days 6 and 12 of differentiation (Figure 2B). These three methods did not show much difference in *T* expression at day 2; however, method Z significantly increased *TBX6*, *PAX3*, *PARAXIS*, and *DMRT2* expression at days 6 or 12 of the differentiation (Figure 2C). Previously, we demonstrated that the addition of basic fibroblast growth factor (bFGF), hepatocyte growth factor (HGF), and insulin growth factor 1 (IGF-1) to serum-free medium could promote myogenic differentiation from paraxial mesoderm in mouse embryonic stem cell differentiation culture (Sakurai et al., 2009). To induce myogenic differentiation, after 12 days differentiation, cells from each method were passaged to Matrigel-coated 6-well plates (40,000 cells/well) and stimulated by SFO3 medium supplemented with 10 ng/mL bFGF, 10 ng/mL IGF, and 10 mg/mL HGF (Figure S2D). Method Z produced more myogenic cells at day 38 of the differentiation (Figures 2D and 2E). The myogenic differentiation efficiency was well correlated with the induction of PAX3+CD271− in each method (Figures 2B and 2E). Furthermore, method Z remarkably increased both myogenic progenitor marker (*MYF5*) gene expression at day 19 and skeletal muscle marker (*MYH3*, *MYOD1*, *MYOG*) gene expression at day 38 (Figure S2E). To conclude, using a PAX3-GFP reporter line, we optimized an induction method to differentiate a dermomyotome-like lineage from hiPSCs using CDMi supplemented with 10 μM CHIR and 5 μM SB with higher efficiency than previous reports.

Myogenic Induction from Dermomyotome-like Lineage

Next, we analyzed the property of the myocytes differentiated from the dermomyotome-like lineage cells (Figure 3A). PAX3-GFP-positive dermomyotome-like cells differentiated into infant myotubes expressing PAX3-GFP by around day 35 (Figure S3A). After the emergence of infant myotubes, the culture medium was switched to conventional muscle maturation medium based on the low concentration of horse serum to mature the myotubes (Neville et al., 1997) (Figure 3A). At around 8 weeks of differentiation, PAX3-GFP-negative mature myotubes were observed in the culture (Figure S3B). These mature myotubes expressed myosin heavy chain and had MYOG-positive multi-nuclei (Figure S3C). After 10 weeks of differentiation, spontaneous twitching was observed (Video S1), which indicates mature myotube formation. According to these data, we successfully developed a step-wise myogenic differentiation protocol from hiPSCs to mature myotubes via dermomyotome-like lineage (Figures 1A and 3A).

Myogenic Lineage Tracing by Monitoring MYF5 Expression

Next, we generated a MYF5-tdTomato reporter hiPSC line to visualize myogenic specification in the differentiation culture using the CRISPR/Cas9 system (Figure S4A). We obtained two heterozygous targeted clones (C3 and E16) (Figure S4B) and one homozygous clone (A24). Upon applying the myogenic differentiation protocol to MYF5-tdTomato C3 hiPSCs, we detected tdTomato-positive cells by flow cytometry after 4 weeks of differentiation in these three clones (Figures 3B and S4C). The MYF5 expression in tdTomato-positive cells was confirmed by RT-PCR (Figure S4D). During the myogenic differentiation, MYF5-tdTomato-positive cells gradually increased and peaked around 20% after 10 weeks of differentiation (Figure 3B). The MYF5-tdTomato-positive cells made a cluster in the early differentiation stage (Figures 3C and S5, upper panel), but were observed diffusely and surrounded by myotubes in the late differentiation stage (Figure 3C and S5, lower panel). Next, we assessed the *in vitro* myogenic differentiation potential of MYF5-tdTomato-positive and -negative cells. In the early differentiation stage, MYF5-tdTomato-positive

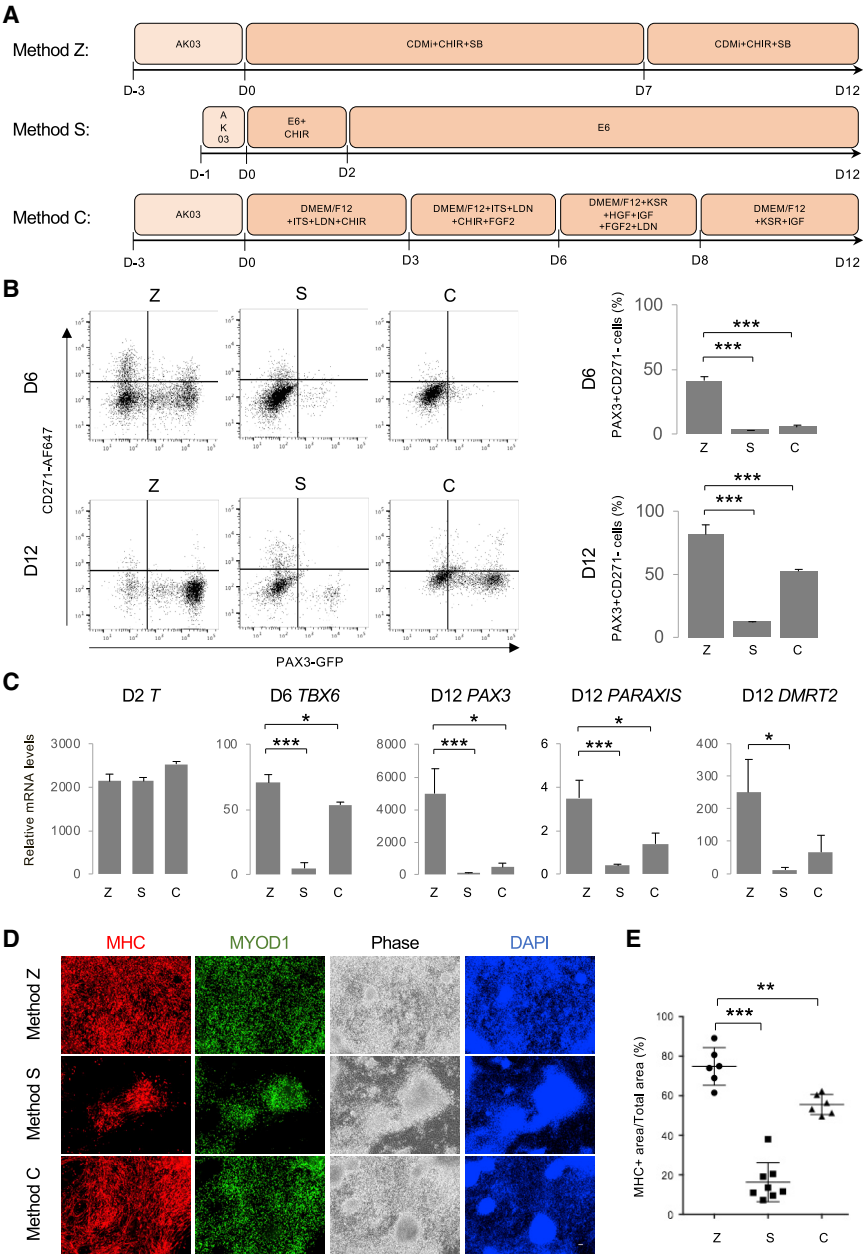

Figure 2. Comparison of the Dermomyotome Differentiation from hiPSCs with Published Methods

(A) Timeline of the dermomyotome differentiation using method Z (Zhao et al. this work), method S (Shelton et al., 2014), and method C (Chal et al., 2015).

(B) Fluorescence-activated cell sorting (FACS) analysis of PAX3 and CD271 at day 6 (D6) and day 12 (D12) of the differentiation. The histogram shows the ratio of PAX3+CD271− cells in the whole cell population. Data of more than three independent experiments are shown as means ± SD. ***p < 0.001.

(C) Time course of the mRNA expression of *BRACHYURY (T)*, *TBX6*, *PAX3*, *PARAXIS*, and *DMRT2* during the dermomyotome differentiation using method Z, method S, and method C. Data of more than three independent experiments are shown as means ± SD. *p < 0.05, ***p < 0.001.

(D) After 12 days of differentiation, cells were passaged on Matrigel-coated plates at the same cell density and stimulated with myogenic differentiation using SF03 medium supplemented with 10 ng/mL bFGF, 10 ng/mL IGF, and 10 mg/mL HGF until day 38. Immunohistochemistry of myosin heavy chain (MHC), MYOD1, and DAPI. Scale bars, 50 μm.

(E) Percentage of the MHC+ area to the whole culture area. Data of more than three independent experiments are shown as means ± SD. n = 6–8; *p < 0.05, **p < 0.01, ***p < 0.001.

cells demonstrated robust myogenic potential, while the MYF5-tdTomato-negative cells showed limited myogenic differentiation (Figure 3D), suggesting that MYF5 is a suitable marker for the purification of myogenic progenitors in the early stage. On the other hand, in the late differentiation stage, both MYF5-tdTomato-positive and -negative cells showed robust myogenic differentiation potential (Figure 3E). Gene expression profiling of myogenic marker genes was carried out to characterize the MYF5-tdTomato-positive cells. *MYF5* expression was confirmed for the quality of the mRNA samples from the purified cells (Figure 3F). *PAX3* was detected highly in the MYF5-tdTomato-positive population at the early differentiation period, but gradually decreased with differentiation (Figure 3F). On the other hand, the satellite cell marker, *PAX7*, was expressed dominantly in the late-stage MYF5-tdTomato-positive population and gradually increased with differentiation (Figure 3F). No significant difference in the expression of the myogenic master regulator *MYOD1* was seen between the MYF5-tdTomato-positive and -negative populations at 12 weeks differentiation (Figure 3F). Intriguingly, a differentiated myocyte marker, *MYOG*, was expressed more in

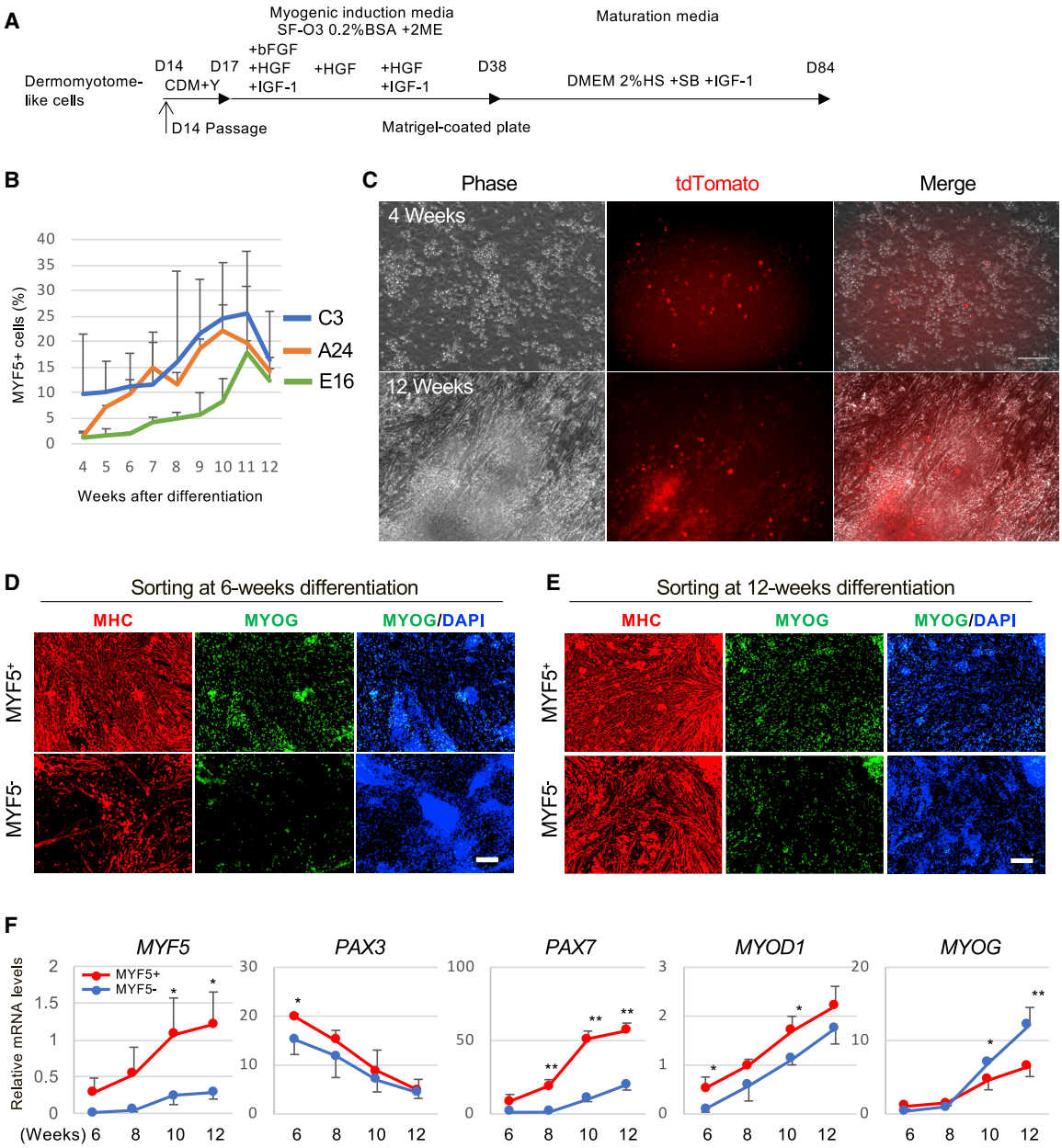

Figure 3. Myogenic Induction from Dermomyotome Lineage

(A) Schematic representation of the myogenic induction and skeletal muscle maturation. Dermomyotome-like cells derived from hiPSCs were plated as single cells in Matrigel-coated plates cultured in CDMi supplemented with 10 μM Y-27632 for 3 days. The medium was changed to SFO3 (0.2% BSA, 0.1 mM 2-ME) supplemented with 10 ng/mL bFGF, 10 ng/mL HGF, and 10 ng/mL IGF-1. After 1 more week of culture, the medium was changed to SFO3 supplemented with 10 ng/mL HGF. After an additional week of culture, the medium was changed to SFO3 supplemented with 10 ng/mL HGF and 10 ng/mL IGF-1. On differentiation day 38, the medium was changed to DMEM supplemented with 2% HS, 5 μm SB 431542, and 10 ng/mL IGF-1 until day 84.

(B) The time course of MYF5+ cells during the differentiation in C3, E16, and A24 cell lines as determined by FACS. Data of three independent experiments are shown as means ± SD.

(C) Representative bright-field (Phase, Ph) and tdTomato images of live cultures of MYF5-tdTomato cells at 4 and 12 weeks in C3 cell line.

(D and E) MYF5+ and MYF5− cells were sorted by FACS at 6 weeks (D) and 12 weeks (E) of differentiation, then plated on a Matrigel-coated plate. MHC, MYOG, and DAPI were detected by immunohistochemistry at 14 days after sorting. Scale bars, 50 μm.

(F) Time course of the mRNA expression of *MYF5*, *PAX3*, *PAX7*, *MYOD1*, and *MYOG* in sorted MYF5+ and MYF5− cells during differentiation from 6 to 12 weeks. Data of three independent experiments are shown as means ± SD. *p < 0.05, **p < 0.01, versus MYF5− cells.

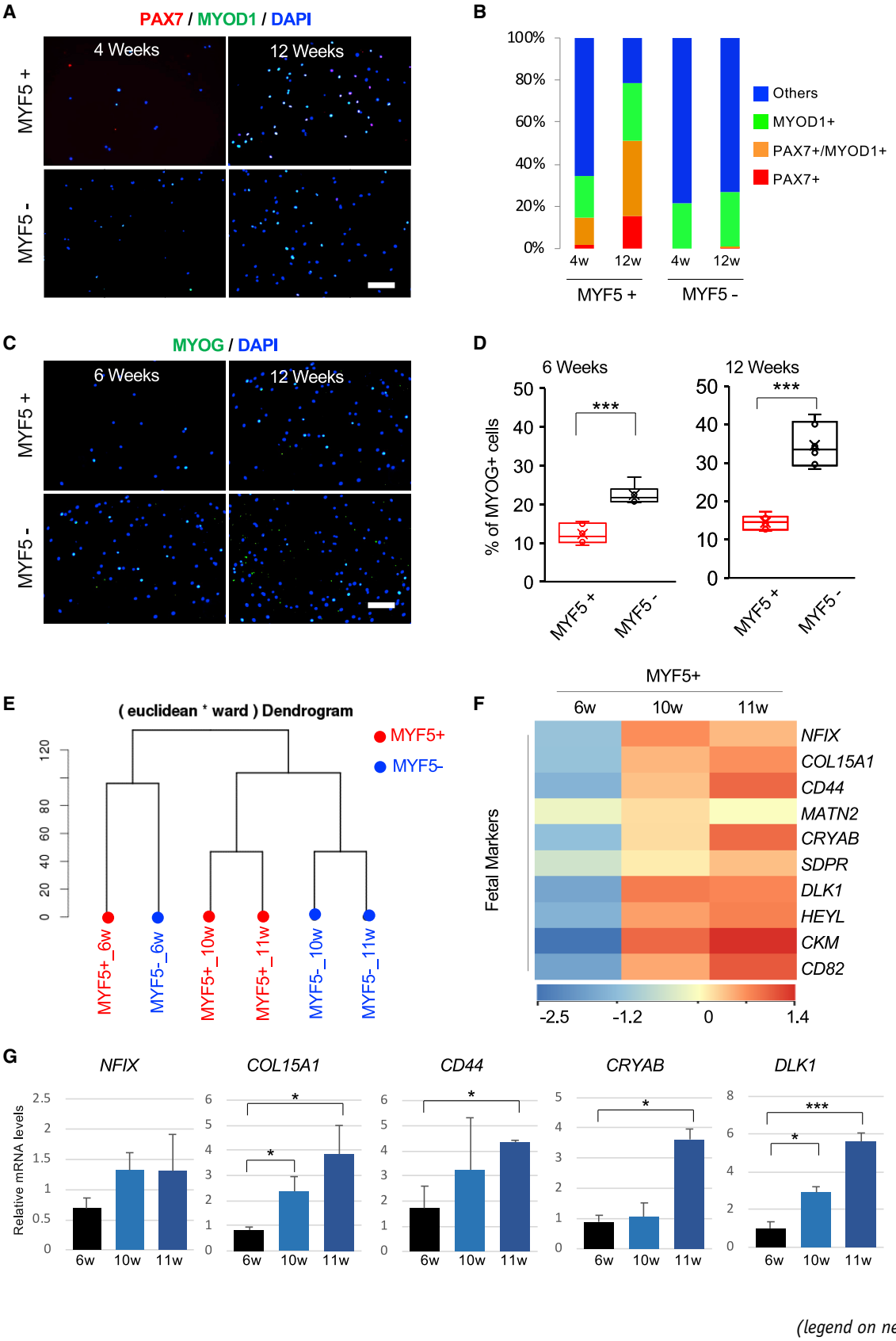

(legend on next page)

the late-stage MYF5-tdTomato-negative population than the late-stage positive population (Figure 3F). These data suggest that the characteristics of the MYF5-tdTomato-positive and -negative populations vary from early differentiation to late differentiation.

Comparison of Myogenic Marker Expression between Early- and Late-Stage Cells

Next, we conducted an immunocytochemistry assay to analyze myogenic marker expressions at the protein level in the MYF5-tdTomato-positive and -negative populations (Figures 4A and 4B). Approximately 15% of the early-stage and 50% of the late-stage MYF5-tdTomato-positive population were positive for PAX7-positive cells (Figures 4A and 4B). On the other hand, the MYF5-tdTomato-negative population contained almost no PAX7-positive cells at any time (Figures 4A and 4B). It is possible that these cells contain differentiated myocytes, which were initially MYF5 positive and subsequently downregulated this gene with proceeding differentiation. To identify differentiated myocytes, MYOG expressions were analyzed (Figures 4C and 4D). The MYF5-tdTomato-negative population contained significantly more MYOG-positive cells than the MYF5-tdTomato-positive population both in early and later stages (Figures 4C and 4D). The proportion of MYOG-positive cells was increased from 22% to 35% in the MYF5-tdTomato-negative population during differentiation. Taken together with the observation that the late-stage MYF5-tdTomato-negative population also showed robust myogenic differentiation potential (Figure 3E), the late-stage MYF5-tdTomato-negative population contains differentiated myogenic cells rather than myogenic progenitor cells.

Notably, PAX7-positive MuSC-like cells were dominantly detected in the MYF5-tdTomato-positive population at late-stage differentiation. Intriguingly, a dendrogram of comprehensive mRNA expression profiling by RNA sequencing (RNA-seq) showed that late-stage MYF5-tdTomato-positive cells clustered nearer to late-stage MYF5-tdTomato-negative cells than to early-stage MYF5-tdTomato-positive cells (Figure 4E). The transcription factor *NFIX* is a fetal-specific transcription factor in developing skeletal muscle (Messina et al., 2010). A later study identified a number of differentially expressed genes between embryonic and fetal muscle progenitor cells (Mourikis et al., 2012). Based on those studies, we compared embryonic and fetal marker genes expressions between early- and late-stage MYF5-tdTomato-positive cells and found that fetal marker genes were highly expressed in late-stage MYF5-tdTomato-positive cells (Figures 4F and 4G), whereas embryonic marker genes were highly expressed in early-stage MYF5-tdTomato-positive cells (Figure S4E). In hiPSCs induced toward myogenic differentiation, MYF5-positive cells adopted a fetal phenotype while concomitantly losing embryonic molecular markers, indicating that the characteristics of MYF5-positive cells depends on the stage of differentiation.

Muscle Regeneration Potential of MYF5-tdTomato-Positive Cells

To assess their muscle regeneration potential, MYF5-tdTomato-positive and -negative cells were purified, and 3×10^5 cells of each population were transplanted into the cardiotoxin-treated tibialis anterior (TA) muscles of immunodeficient mice (Figure 5). Although MYF5-tdTomato-positive cells both at the early and late stage of differentiation showed muscle regeneration potential based on the detection of human SPECTRIN-positive mouse muscle fibers, including human nuclei (Figures 5A and 5B), the number of SPECTRIN-positive muscle fibers was much higher with the late-stage cell transplantation (Figure 5C). These results suggest that late-stage MYF5-tdTomato-positive cells have higher muscle regeneration potential than early-stage cells *in vivo*. In contrast, MYF5-tdTomato-negative cells of all differentiation stages showed almost no muscle regeneration (Figures 5A and 5B). When MYF5-tdTomato-negative cells were transplanted, engrafted cells were only detected in the interstitial area of the muscles and formed cyst-like structures (Figures 5A and 5B). These engrafted human cells in the interstitial area were negative

Figure 4. Comparison of Myogenic Marker Expression between Early- and Late-Stage Differentiation

(A) Immunocytochemistry of PAX7+ and MYOD1+ in sorted MYF5+ and MYF5− cells at 4 or 12 weeks of differentiation. Scale bar, 50 μm.

(B) Branching index of PAX7+, MYOD1+, and MYOD1+PAX7+ cells in sorted MYF5+ and MYF5− cells. Data shown are from three biological replicates.

(C) Immunocytochemistry of DAPI and MYOG in sorted MYF5+ and My5− cells at 6 and 12 weeks of differentiation. Scale bar, 50 μm.

(D) The box diagram shows the percentage of MYOG+ in DAPI+ cells. Data of three independent experiments are shown as means ± SD. ***p < 0.001 using Student's t test.

(E) Ward's linkage using Euclidean distances.

(F) Heatmap of fetal marker gene expression in MYF5+ cells differentiated for 6, 10, or 11 weeks (green is low expression and red is high expression).

(G) Bar charts indicate the relative transcript levels of fetal markers in MYF5+ cells at 6, 10, and 11 weeks by qPCR. Data of three independent experiments are shown as means ± SD. *p < 0.05, ***p < 0.001 using one-way ANOVA.

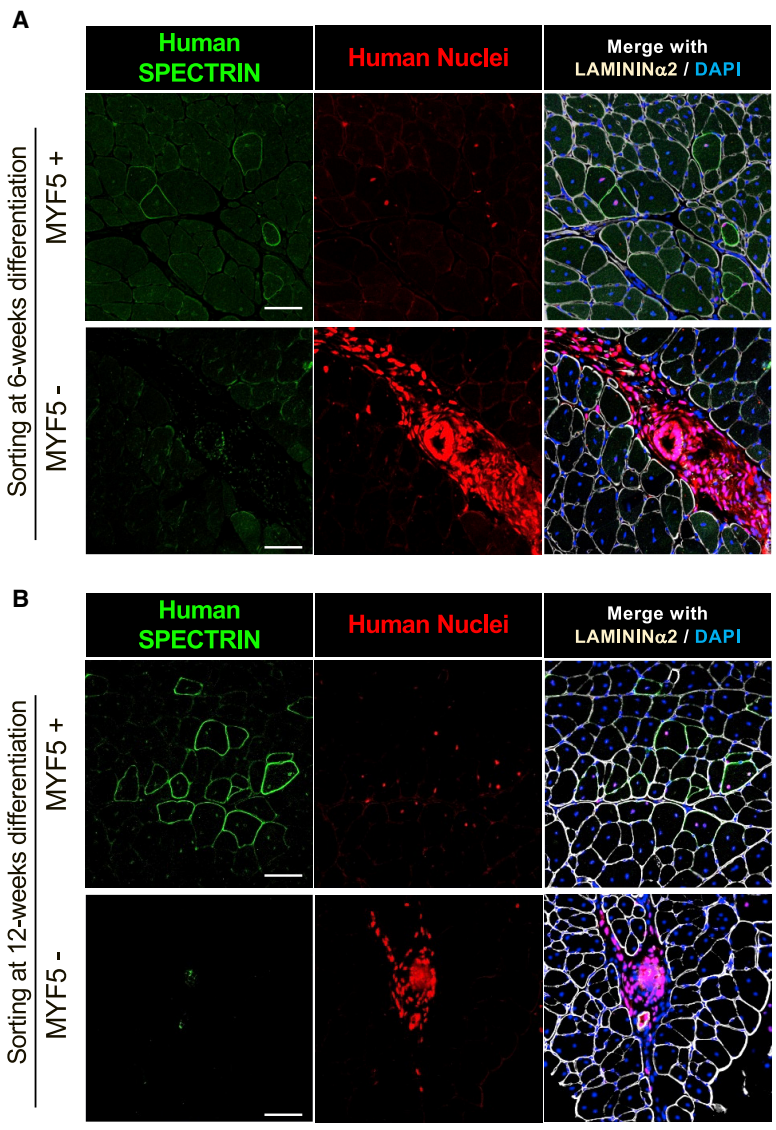

Figure 5. Muscle Regeneration Potential of MYF5-tdTomato+ Cells

Sorted MYF5+ or MYF5− cells were transplanted into the cardiotoxin-treated TA muscles of immunodeficient mice, and the engrafted cells were evaluated by immunohistochemistry 4 weeks after the transplantation. Immunohistochemistry of human SPECTRIN (green), human nuclei (red), LAMININ α2 (white), and DAPI (blue) in sorted 6-week differentiated (A) and 12-week differentiated (B) MYF5+/− cells. Scale bars, 50 μm. (C) Graphs quantifying the number of engrafted myofibers in one TA muscle. Data of three independent experiments are shown as means ± SD. *$p < 0.05$ using one-way ANOVA.

for both MYOD1 and MYOG (Figure S6). Furthermore, very few SPECTRIN-positive muscle fibers were detected (Figure 5C). These results demonstrate that muscle progenitor cells with muscle regeneration potential can be purified by MYF5 expression during the induction of myogenic differentiation in hiPSCs.

DYSTROPHIN Restoration by MYF5-tdTomato-Positive Cell Transplantation in DMD Model Mice

Subsequently, we assessed the DYSTROPHIN restoration potential of MYF5-tdTomato-positive cells by transplanting them into DMD-null/NSG model mice (Figure 6). Many reports have demonstrated DYSTROPHIN restoration by hiPSC-derived muscle progenitor engraftment. However, most did so after inducing muscle injury by cardiotoxin injection or forced running before the cell transplantation to enhance the engraftment. However, those pretreatments should be avoided in clinical application. Therefore, no pretreatment was done in our transplantation study. Based on the results of Figure 5, we used late-stage MYF5-tdTomato-positive cells for the cell transplantation. We found human LAMIN A/C-positive nuclei were mainly detected in host muscle fibers that were DYSTROPHIN positive (Figure 6A), suggesting that MYF5-tdTomato-positive cells at 12 weeks differentiation robustly regenerated the muscle of DMD-null/NSG mice. More than 100 DYSTROPHIN-positive muscle fibers were regenerated on average at 4 weeks after the transplantation (Figure 6B). At 2 weeks after transplantation, DYSTROPHIN-positive muscle fibers were smaller than normal muscle fibers, and many transplanted human cells exited the interstitial area of the muscle (Figure S7A). At 3 months after transplantation, the size of the DYSTROPHIN-positive fibers was comparable with the host myofibers, and the transplanted cells in the interstitial area had dramatically decreased (Figure S7A). On the other hand, MYF5-tdTomato-negative cells engrafted in the interstitial area of muscle fibers formed cyst-like structures even in the muscle of DMD model mice (Figure 6A) with very few DYSTROPHIN-positive muscle fibers (Figure 6B). Although MYF5-tdTomato-positive cells were engrafted as myonuclei, indicating their location within the DYSTROPHIN-positive membrane, several engrafted cells were located outside the DYSTROPHIN-positive plasma membrane and inside the LAMININ α2-positive basement membrane, which has been reported as the specific position of muscle satellite cells (Mauro, 1961) (Figure 6C, white arrowheads). Some human LAMIN A/C-positive engrafted cells expressed PAX7 (Figure 6D), indicating that some engrafted MYF5-tdTomato-positive cells distributed spatially like satellite cells. Approximately 4% of human nuclei were located in the specific niche position (data not shown). Moreover, MYOD1 expression indicated that some human LAMIN A/C-positive cells were located outside of the muscle fibers at 4 weeks after transplantation (Figure 6E). These MYF5-tdTomato-positive cell-derived MYOD1-positive cells were sometimes located near the embryonic-type myosin heavy chain 3 (MYH3)-positive regenerating myofibers (Figure S7B), suggesting that repeated muscle regeneration might occur by human myoblasts expanded from the engrafted hiPSC-derived MuSCs.

Functional Recovery of DMD Model Mice after DYSTROPHIN Restoration

Finally, we assessed the functional feature of DMD-null/NSG mice after the MYF5-tdTomato-positive cell transplantation. We used a muscle contraction force assessment system on living mice with anesthesia for the assessment. One to two million MYF5-tdTomato-positive cells were transplanted into the right gastrocnemius of DMD-null/NSG mice, and maximum muscle contraction force of both sides of the gastrocnemius was analyzed at 2, 4, and 6 weeks after the transplantation. No difference in muscle force between the two sides was detected at 2 and 4 weeks after transplantation (data not shown), but a slight but nevertheless significant increase in force was detected in all three transplanted gastrocnemius muscles compared with the contralateral sham-operated muscles at 6 weeks (Figure 7). These results suggest that the restoration of DYSTROPHIN-positive muscle fibers could contribute to the amelioration of muscle function in DMD model mice.

DISCUSSION

In this study, we succeeded in identifying MuSCs derived from hiPSCs following myogenic developmental steps. Our results reveal the following three main points. First, the long-term application of high-concentration WNT agonists induces dermomyotome cells in more than 90% of differentiated cells. Second, the characteristics of the MYF5-positive cells vary between the early and late differentiation stages. During the differentiation process, MYF5-tdTomato-positive cells gradually mature and finally acquire characteristics resembling fetal MuSCs. Third, late-stage MYF5-tdTomato-positive cells have muscle regeneration potential, which recovers DYSTROPHIN and improves muscular function of the limbs that received the transplant in DMD-null/NSG model mice. We propose that these late-stage MYF5-positive cells should be explored for their cell therapy potential in DMD.

To induce dermomyotome-like cells, a lower dose or short exposure time of a WNT agonist was used in previous reports (Chal et al., 2015, 2016; Choi et al., 2016; Hicks et al., 2018; Shelton et al., 2014). In this study, however, we optimized a long-term protocol with a higher WNT

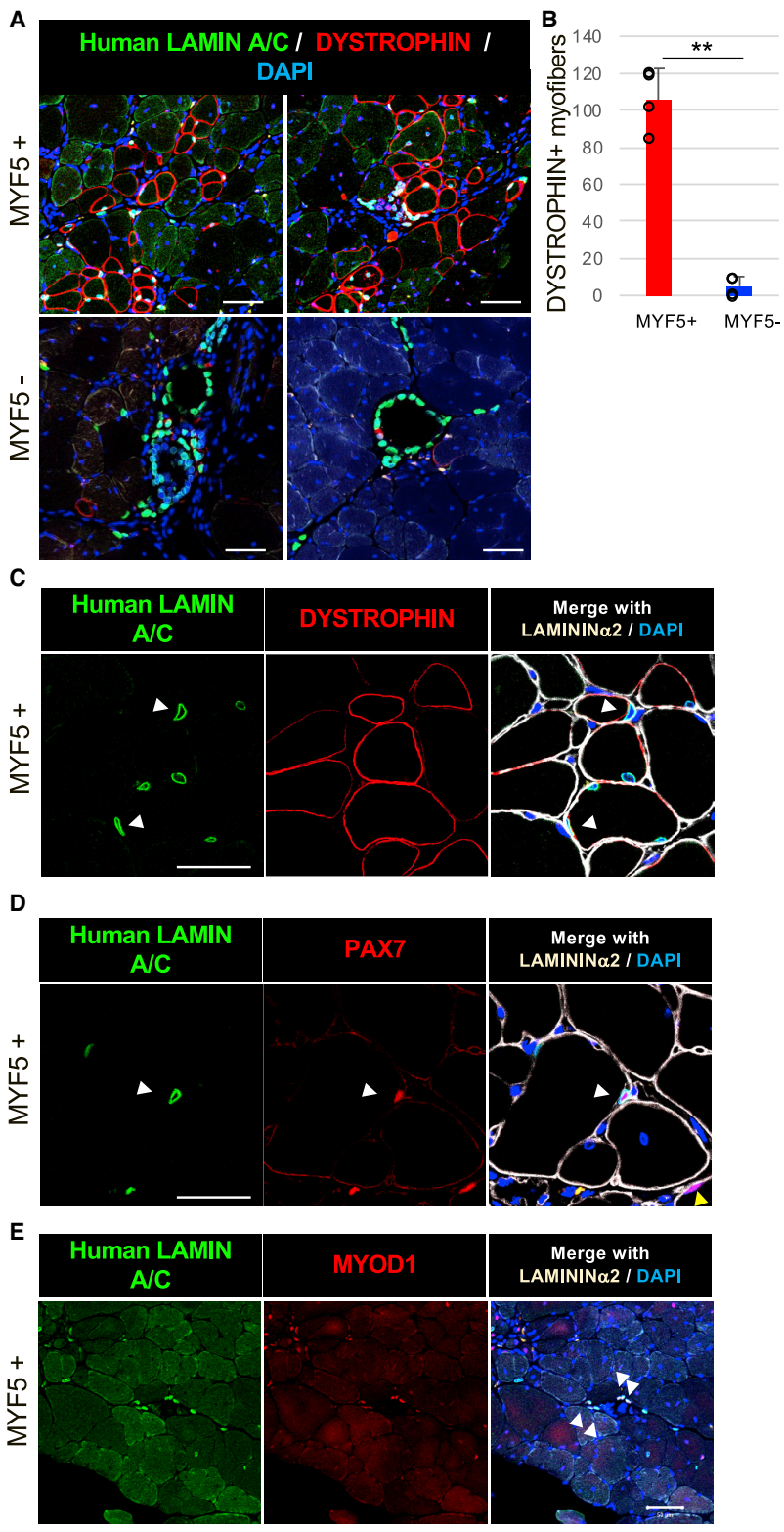

Figure 6. DYSTROPHIN Restoration by MYF5-tdTomato+ Cell Transplantation in DMD Model Mice

Sorted MYF5+ or MYF5− cells were transplanted into the TA muscles of DMD-null/NSG model mice, and the engrafted cells were evaluated by immunohistochemistry 4 weeks after the transplantation.

(A) Immunohistochemistry of human LAMIN A/C (green), DYSTROPHIN (red), and DAPI (blue) in sorted 12-week differentiated MYF5+/− cells. Left and right images show different positions of the muscles under the same conditions. Magnification, 200×.

(B) Number of engrafted myofibers in one TA muscle. Data of four independent experiments are shown as means ± SD. **$p < 0.01$ using Student's t test.

(C) Immunohistochemistry of human LAMIN A/C (green), DYSTROPHIN (red), LAMININ α2 (white), and DAPI (blue) in sorted 12-week differentiated MYF5+/− cells. White arrowheads show human nuclei inside the LAMININ α2+ basement membrane and outside the DYSTROPHIN+ plasma membrane. Magnification, 400×.

(D) Immunohistochemistry of human LAMIN A/C (green), PAX7 (red), LAMININ α2 (white), and DAPI (blue) in sorted 12-week differentiated MYF5+/− cells. White arrowheads show that engrafted human LAMIN A/C+ cells were also PAX7+ cells. Magnification, 400×.

(E) Immunohistochemistry of human LAMIN A/C (green), MYOD1 (red), LAMININ α2 (white), and DAPI (blue) in sorted 12-week differentiated MYF5+/− cells. White arrowheads show that engrafted human LAMIN A/C+ cells were also MYOD1+ cells. Magnification, 200×. Scale bars, 50 μm.

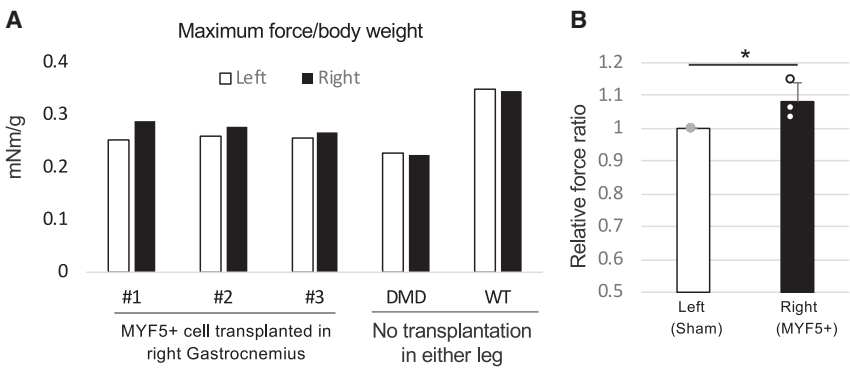

Figure 7. Functional Recovery of DMD Model Mice after DYSTROPHIN Restoration

(A) Maximum muscle force of MYF5+ cell-transplanted leg (right) and sham leg (left) in DMD mouse. The maximum force of the sham was used as the control.

(B) Maximum muscle force of the MYF5+-transplanted leg relative to the shammed leg. Data of three independent experiments are shown as means ± SD. *$p < 0.05$ using Student's t test.

agonist dose. The induction efficiency of PAX3+ CD271− cells was 45% at day 6 and 90% at day 12, which was significantly higher than previous reports. These results suggest that dermomyotome-like cell populations continue to increase with exposure to the WNT agonist. Moreover, if the induction medium was converted to myogenic differentiation medium within the first 8 days of the protocol, then almost no MYF5-tdTomato-positive cells were detected in the following stage (data not shown). Thus, we consider the marked increase of the differentiation efficiency of dermomyotome cells important for myogenic differentiation.

Comprehensive analysis of the transcriptome revealed that early- and late-stage MYF5-tdTomato-positive cells are markedly distinct, with late-stage MYF5-tdTomato-positive cells more resembling late-stage MYF5-tdTomato-negative cells. Early-stage MYF5-tdTomato-positive cells highly expressed *PAX3* and embryonic markers, but weakly expressed *PAX7* and fetal markers, suggesting that these cells are embryonic myogenic progenitor cells (Mourikis et al., 2012; Relaix et al., 2005). After 10–12 weeks of differentiation, however, these cells decreased their expression of *PAX3* and gradually increased their expression of *PAX7* and *MYOD1*, and increased their expression of fetal markers, suggesting a similarity with fetal MuSCs (Kuang et al., 2006; Mourikis et al., 2012; Oustanina et al., 2004; Seale et al., 2000). In human development, characterization of human fetal MCAM-positive cells in skeletal muscle demonstrated that CD82 is the marker of fetal muscle progenitors (Alexander et al., 2016). In their dataset, we identified that *COL15A1*, *CRYAB*, *DLK1*, and *CD82* were well correlated to our RNA-seq data, suggesting that some of the characteristics of fetal MuSCs are conserved between mouse and human. Furthermore, we found that late-stage MYF5-tdTomato-positive cells localized near myocytes and myotubes. Thus, we hypothesize that myocytes and myotubes might provide an essential niche for the induction of MuSCs. Further research is needed to determine both the origin and the niche of MuSCs in the hiPSC differentiation culture. In contrast, we found that the late-stage MYF5-tdToamto-negative population expressed MYOG dominantly, suggesting that the MYF5-tdTomato-negative cells were mainly composed of differentiated myocytes that might have once expressed MYF5 in the early stage. Furthermore, while up to 40% of the MYF5-tdTomato-negative cells were MYOG positive, approximately half of the cells were non-myogenic cells. Since the MYOG expression promotes cell-cycle withdrawal (Andrés and Walsh, 1996), these differentiated myocytes could hardly contribute to muscle regeneration. The last non-myogenic cells in the MYF5-tdTomato-negative population were composed of neural cells, mesenchymal cells, and so on (data not shown). Most of the engrafted cells from MYF5-tdTomato-negative cells were non-myogenic cells, suggesting that the engrafted cells might be mainly derived from non-myogenic cells rather than from post-mitotic differentiated myocytes.

Among reported hiPSC-derived MuSCs, iPAX7 is believed to fuse to host muscles in DMD model mice most effectively (Darabi et al., 2012). Muscle progenitors prepared using a transgene-free method have lower regenerative potential, and PAX7 overexpression in the progenitors is reported to enhance their regenerative potential (Kim et al., 2017). Our transgene-free protocol, on the other hand, has comparable regeneration potential as transgene protocols. Differentiating hiPSCs to MuSCs, which we defined as late-stage MYF5-positive cells, resulted in fusion with more than 100 muscle fibers in DMD model mice and converting the fibers to DYSTROPHIN-positive by a single administration.

Notably, most previous studies induced muscle injury by cardiotoxin injection as a pretreatment (Darabi et al., 2012; Choi et al., 2016; Hicks et al., 2018; Barberi et al., 2007) to enhance the fusion efficiency of the engrafted cells (Darabi et al., 2008). However, such an invasive pretreatment is not applicable clinically. In contrast, our method based on no pretreatment is more consistent with clinical conditions in which the patient will not undergo a treatment to induce the muscle damage.

In conclusion, we developed a novel method in which hiPSCs are differentiated into MuSCs by recapitulating myogenic developmental steps. We found that the resultant MuSCs, which were marked by MYF5 expression at the late stage of the differentiation protocol, have high regeneration potential in DMD model mice. Further optimization of the protocol, namely purification using cell surface markers instead of the MYF5 reporter line, using clinical iPSC stocks and evaluation of the long-term safety after engraftment, could contribute to an effective cell therapy for DMD and other degenerative muscular diseases.

EXPERIMENTAL PROCEDURES

Ethical Approval

Ethical approval for this study was granted by the Ethics Committee on Human Stem Cell Research, Institute for Frontier Medical Sciences, Kyoto University, and Kyoto University Hospital. All mouse experiments were carried out according to protocols approved by the Animal Research Committee of Kyoto University.

Transplantation Studies

NSG mice were purchased from Charles River Laboratories. Eight- to 10-week-old NSG mice were anesthetized with isoflurane (Abbvie), and 50 μL of 1 μM cardiotoxin (Latoxian) was injected in both TA muscles before intramuscular cell transplantation. Twenty-four hours after the cardiotoxin damage, 3×10^5 of MYF5-tdTomato-positive and -negative cells at 6–12 weeks differentiation were injected into the left TA muscles, while the right TA muscles were used as the sham-operated control. One month after transplantation, mice were sacrificed, and TA muscle samples were collected and analyzed by immunohistochemical staining. NSG mice were also mated with DMD-null mice (Kudoh et al., 2005) to generate DMD-null/NSG mice for the *in vivo* transplantation studies as a DMD model. Five- to 8-week-old DMD-null/NSG mice were anesthetized with isoflurane without any pretreatment, and 3×10^5 of MYF5-tdTomato-positive and -negative cells at 12 weeks differentiation were injected into the left and right TA muscles, respectively. The mice were sacrificed 2, 4, and 12 weeks after transplantation, and TA muscle samples were collected and analyzed by immunohistochemical staining.

Statistical Analysis

For human DYSTROPHIN-positive myofiber data and muscle force data, unpaired Student's t tests were calculated. For human SPECTRIN-positive data and qRT-PCR data, one-way ANOVA was calculated. Differences were considered significant for p values ≤ 0.05.

Other Materials and Methods

Other materials and methods are described in Supplemental Experimental Procedures.

Data and Code Availability

The accession number for the RNA-sequencing data reported in this paper is DDBJ: DRA010291DRA010291.

SUPPLEMENTAL INFORMATION

Supplemental Information can be found online at https://doi.org/10.1016/j.stemcr.2020.06.004.

AUTHOR CONTRIBUTIONS

The study concept was generated by H.S. The experimentation was completed by M.Z., A.T., S.T., N.T.-N., and M.Nalbandian with support from M.Nagai, Y.N., M.Nakasa, Y.I., and T.S. Microarray analysis was performed by S.T. and A.W. The PAX3-GFP reporter cell line was provided by H.S. with support from M.I. The MYF5-tdTomato reporter cell line was established by S.T. with support from A.H. and T.S. The manuscript and figures were prepared by M.Z., A.T., S.T., M.Nalbandian, and H.S. M.Z. and H.S. finally approved this manuscript.

ACKNOWLEDGMENTS

We thank Masae Sato, Yoko Kanamori, and Megumi Goto for technical assistance. We also thank Peter Karagiannis for English proofreading. This work was mainly supported by a grant from The Projects for Technical Development and The Core Center for iPS Cell Research, both of which are programs in Research Center Network for Realization of Regenerative Medicine provided by the Japan Agency for Medical Research and Development, AMED (to H.S.). A part of this research was also supported by Intramural Research Grant 28-6 for Neurological and Psychiatric Disorders of NCNP (to H.S.) and a grant from Acceleration Transformative Research for Medical Innovation Set-up Scheme (ACT-MS) from AMED (to H.S.). A.T. and S.T. are employees of Asahi Kasei Company Limited. A part of this work was supported by a collaboration budget from Asahi Kasei Company Limited.

Received: June 24, 2019
Revised: June 3, 2020
Accepted: June 3, 2020
Published: July 2, 2020

REFERENCES

Albini, S., Coutinho, P., Malecova, B., Giordani, L., Savchenko, A., Forcales, S.V., and Puri, P.L. (2013). Epigenetic reprogramming of human embryonic stem cells into skeletal muscle cells and generation of contractile myospheres. Cell Rep. *3*, 661–670.

Alexander, M.S., Rozkalne, A., Colletta, A., Spinazzola, J.M., Johnson, S., Rahimov, F., Meng, H., Lawlor, M.W., Estrella, E., Kunkel, L.M., et al. (2016). CD82 is a marker for prospective isolation of human muscle satellite cells and is linked to muscular dystrophies. Cell Stem Cell *19*, 800–807.

Andrés, V., and Walsh, K. (1996). MYOG expression, cell cycle withdrawal, and phenotypic differentiation are temporally separable events that precede cell fusion upon myogenesis. J. Cell Biol. *132*, 657–666.

Barberi, T., Bradbury, M., Dincer, Z., Panagiotakos, G., Socci, N.D., and Studer, L. (2007). Derivation of engraftable skeletal myoblasts from human embryonic stem cells. Nat. Med. *13*, 642–648.

Borchin, B., Chen, J., and Barberi, T. (2013). Derivation and FACS-mediated purification of PAX3+/PAX7+ skeletal muscle precursors from human pluripotent stem cells. Stem Cell Reports *1*, 620–631.

Caron, L., Kher, D., Lee, K.L., McKernan, R., Dumevska, B., Hidalgo, A., Li, J., Yang, H., Main, H., Ferri, G., et al. (2016). A human pluripotent stem cell model of facioscapulohumeral muscular dystrophy-affected skeletal muscles. Stem Cells Transl. Med. *5*, 1145–1161.

Cerletti, M., Jurga, S., Witczak, C.A., Hirshman, M.F., Shadrach, J.L., Goodyear, L.J., and Wagers, A.J. (2008). Highly efficient, functional engraftment of skeletal muscle stem cells in dystrophic muscles. Cell *134*, 37–47.

Chal, J., Oginuma, M., Al Tanoury, Z., Gobert, B., Sumara, O., Hick, A., Bousson, F., Zidouni, Y., Mursch, C., Moncuquet, P., et al. (2015). Differentiation of pluripotent stem cells to muscle fiber to model Duchenne muscular dystrophy. Nat. Biotechnol. *33*, 962–969.

Chal, J., Al Tanoury, Z., Hestin, M., Gobert, B., Aivio, S., Hick, A., Cherrier, T., Nesmith, A.P., Parker, K.K., and Pourquie, O. (2016). Generation of human muscle fibers and satellite-like cells from human pluripotent stem cells in vitro. Nat. Protoc. *11*, 1833–1850.

Chapman, D.L., Agulnik, I., Hancock, S., Silver, L.M., and Papaioannou, V.E. (1996). Tbx6, a mouse T-box gene implicated in paraxial mesoderm formation at gastrulation. Dev. Biol. *180*, 532–534.

Choi, I.Y., Lim, H., Estrellas, K., Mula, J., Cohen, T.V., Zhang, Y., Donnelly, C.J., Richard, J.P., Kim, Y.J., Kim, H., et al. (2016). Concordant but varied phenotypes among duchenne muscular dystrophy patient-specific myoblasts derived using a human iPSC-based model. Cell Rep. *15*, 2301–2312.

Darabi, R., Gehlbach, K., Bachoo, R.M., Kamath, S., Osawa, M., Kamm, K.E., Kyba, M., and Perlingeiro, R.C. (2008). Functional skeletal muscle regeneration from differentiating embryonic stem cells. Nat. Med. *14*, 134–143.

Darabi, R., Arpke, R.W., Irion, S., Dimos, J.T., Grskovic, M., Kyba, M., and Perlingeiro, R.C. (2012). Human ES- and iPS-derived myogenic progenitors restore DYSTROPHIN and improve contractility upon transplantation in dystrophic mice. Cell Stem Cell *10*, 610–619.

Fairclough, R.J., Wood, M.J., and Davies, K.E. (2013). Therapy for Duchenne muscular dystrophy: renewed optimism from genetic approaches. Nat. Rev. Genet. *14*, 373–378.

Gilbert, P.M., Havenstrite, K.L., Magnusson, K.E., Sacco, A., Leonardi, N.A., Kraft, P., Nguyen, N.K., Thrun, S., Lutolf, M.P., and Blau, H.M. (2010). Substrate elasticity regulates skeletal muscle stem cell self-renewal in culture. Science *329*, 1078–1081.

Goulding, M.D., Chalepakis, G., Deutsch, U., Erselius, J.R., and Gruss, P. (1991). PAX3, a novel murine DNA binding protein expressed during early neurogenesis. EMBO J. *10*, 1135–1147.

Hashimoto, K., Fujimoto, H., and Nakatsuji, N. (1987). An ECM substratum allows mouse mesodermal cells isolated from the primitive streak to exhibit motility similar to that inside the embryo and reveals a deficiency in the T/T mutant cells. Development *100*, 587–598.

Hicks, M.R., Hiserodt, J., Paras, K., Fujiwara, W., Eskin, A., Jan, M., Xi, H., Young, C.S., Evseenko, D., Nelson, S.F., et al. (2018). ERBB3 and NGFR mark a distinct skeletal muscle progenitor cell in human development and hPSCs. Nat. Cell Biol. *20*, 46–57.

Hoffman, E.P., Knudson, C.M., Campbell, K.P., and Kunkel, L.M. (1987). Subcellular fractionation of DYSTROPHIN to the triads of skeletal muscle. Nature *330*, 754–758.

Kim, J., Magli, A., Chan, S.S.K., Oliveira, V.K.P., Wu, J., Darabi, R., Kyba, M., and Perlingeiro, R.C.R. (2017). Expansion and purification are critical for the therapeutic application of pluripotent stem cell-derived myogenic progenitors. Stem Cell Reports *9*, 12–22.

Kinali, M., Arechavala-Gomeza, V., Feng, L., Cirak, S., Hunt, D., Adkin, C., Guglieri, M., Ashton, E., Abbs, S., Nihoyannopoulos, P., et al. (2009). Local restoration of DYSTROPHIN expression with the morpholino oligomer AVI-4658 in Duchenne muscular dystrophy: a single-blind, placebo-controlled, dose-escalation, proof-of-concept study. Lancet Neurol. *8*, 918–928.

Kuang, S., Charge, S.B., Seale, P., Huh, M., and Rudnicki, M.A. (2006). Distinct roles for PAX7 and PAX3 in adult regenerative myogenesis. J. Cell Biol. *172*, 103–113.

Kudoh, H., Ikeda, H., Kakitani, M., Ueda, A., Hayasaka, M., Tomizuka, K., and Hanaoka, K. (2005). A new model mouse for Duchenne muscular dystrophy produced by 2.4 Mb deletion of DYSTROPHIN gene using Cre-loxP recombination system. Biochem. Biophys. Res. Commun. *328*, 507–516.

Mahmood, A., Harkness, L., Schroder, H.D., Abdallah, B.M., and Kassem, M. (2010). Enhanced differentiation of human embryonic stem cells to mesenchymal progenitors by inhibition of TGF-beta/activin/nodal signaling using SB-431542. J. Bone Miner Res. *25*, 1216–1233.

Marg, A., Escobar, H., Gloy, S., Kufeld, M., Zacher, J., Spuler, A., Birchmeier, C., Izsvak, Z., and Spuler, S. (2014). Human satellite cells have regenerative capacity and are genetically manipulable. J. Clin. Invest. *124*, 4257–4265.

Mauro, A. (1961). Satellite cell of skeletal muscle fibers. J. Biophys. Biochem. Cytol. *9*, 493–495.

Messina, G., Biressi, S., Monteverde, S., Magli, A., Cassano, M., Perani, L., Roncaglia, E., Tagliafico, E., Starnes, L., Campbell, C.E., et al. (2010). Nfix regulates fetal-specific transcription in developing skeletal muscle. Cell *140*, 554–566.

Montarras, D., Morgan, J., Collins, C., Relaix, F., Zaffran, S., Cumano, A., Partridge, T., and Buckingham, M. (2005). Direct isolation of satellite cells for skeletal muscle regeneration. Science *309*, 2064–2067.

Mourikis, P., Gopalakrishnan, S., Sambasivan, R., and Tajbakhsh, S. (2012). Cell-autonomous Notch activity maintains the temporal specification potential of skeletal muscle stem cells. Development *139*, 4536–4548.

Muntoni, F., and Wood, M.J. (2011). Targeting RNA to treat neuromuscular disease. Nat. Rev. Drug Discov. *10*, 621–637.

Nakajima, T., Shibata, M., Nishio, M., Nagata, S., Alev, C., Sakurai, H., Toguchida, J., and Ikeya, M. (2018). Modeling human somite development and fibrodysplasia ossificans progressiva with

induced pluripotent stem cells. Development *145*. https://doi.org/10.1242/dev.165431.

Negroni, E., Riederer, I., Chaouch, S., Belicchi, M., Razini, P., Di Santo, J., Torrente, Y., Butler-Browne, G.S., and Mouly, V. (2009). In vivo myogenic potential of human CD133+ muscle-derived stem cells: a quantitative study. Mol. Ther. *17*, 1771–1778.

Neville, C., Rosenthal, N., McGrew, M., Bogdanova, N., and Hauschka, S. (1997). Skeletal muscle cultures. Methods Cell Biol. *52*, 85–116.

Nord, H., Nygard Skalman, L., and von Hofsten, J. (2013). Six1 regulates proliferation of PAX7-positive muscle progenitors in zebrafish. J. Cell Sci. *126*, 1868–1880.

Nowak, K.J., and Davies, K.E. (2004). Duchenne muscular dystrophy and DYSTROPHIN: pathogenesis and opportunities for treatment. EMBO Rep. *5*, 872–876.

Oustanina, S., Hause, G., and Braun, T. (2004). PAX7 directs postnatal renewal and propagation of myogenic satellite cells but not their specification. EMBO J. *23*, 3430–3439.

Rao, L., Tang, W., Wei, Y., Bao, L., Chen, J., Chen, H., He, L., Lu, P., Ren, J., Wu, L., et al. (2012). Highly efficient derivation of skeletal myotubes from human embryonic stem cells. Stem Cell Rev. Rep. *8*, 1109–1119.

Rao, L., Qian, Y., Khodabukus, A., Ribar, T., and Bursac, N. (2018). Engineering human pluripotent stem cells into a functional skeletal muscle tissue. Nat. Commun. *9*, 126.

Relaix, F., Rocancourt, D., Mansouri, A., and Buckingham, M. (2005). A PAX3/PAX7-dependent population of skeletal muscle progenitor cells. Nature *435*, 948–953.

Sacco, A., Doyonnas, R., Kraft, P., Vitorovic, S., and Blau, H.M. (2008). Self-renewal and expansion of single transplanted muscle stem cells. Nature *456*, 502–506.

Sakurai, H., Inami, Y., Tamamura, Y., Yoshikai, T., Sehara-Fujisawa, A., and Isobe, K. (2009). Bidirectional induction toward paraxial mesodermal derivatives from mouse ES cells in chemically defined medium. Stem Cell Res. *3*, 157–169.

Sato, T., Rocancourt, D., Marques, L., Thorsteinsdottir, S., and Buckingham, M. (2010). A PAX3/Dmrt2/MYF5 regulatory cascade functions at the onset of myogenesis. PLoS Genet. *6*, e1000897.

Seale, P., Sabourin, L.A., Girgis-Gabardo, A., Mansouri, A., Gruss, P., and Rudnick, M.A. (2000). PAX7 is required for the specification of myogenic satellite cells. Cell *102*, 777–786.

Shelton, M., Metz, J., Liu, J., Carpenedo, R.L., Demers, S.P., Stanford, W.L., and Skerjanc, I.S. (2014). Derivation and expansion of PAX7-positive muscle progenitors from human and mouse embryonic stem cells. Stem Cell Reports *3*, 516–529.

Shoji, E., Sakurai, H., Nishino, T., Nakahata, T., Heike, T., Awaya, T., Fujii, N., Manabe, Y., Matsuo, M., and Sehara-Fujisawa, A. (2015). Early pathogenesis of Duchenne muscular dystrophy modelled in patient-derived human induced pluripotent stem cells. Sci. Rep. *5*, 12831.

Takahashi, K., Tanabe, K., Ohnuki, M., Narita, M., Ichisaka, T., Tomoda, K., and Yamanaka, S. (2007). Induction of pluripotent stem cells from adult human fibroblasts by defined factors. Cell *131*, 861–872.

Tanaka, K.K., Hall, J.K., Troy, A.A., Cornelison, D.D., Majka, S.M., and Olwin, B.B. (2009). Syndecan-4-expressing muscle progenitor cells in the SP engraft as satellite cells during muscle regeneration. Cell Stem Cell *4*, 217–225.

Tierney, M.T., Gromova, A., Sesillo, F.B., Sala, D., Spenle, C., Orend, G., and Sacco, A. (2016). Autonomous extracellular matrix remodeling controls a progressive adaptation in muscle stem cell regenerative capacity during development. Cell Rep. *14*, 1940–1952.

Tremblay, J.P. (2006). CSCI/RCPSC Henry Friesen Lecture: cell therapy for Duchenne muscular dystrophy. Clin. Invest. Med. *29*, 378–382.

White, S., Kalf, M., Liu, Q., Villerius, M., Engelsma, D., Kriek, M., Vollebregt, E., Bakker, B., Ommen, G.-J.B.V., Breuning, M.H., et al. (2002). Comprehensive detection of genomic duplications and deletions in the DMD gene, by use of multiplex amplifiable probe hybridization. Am. J. Hum. Genet. *71*, 365–374.

Xu, X., Wilschut, K.J., Kouklis, G., Tian, H., Hesse, R., Garland, C., Sbitany, H., Hansen, S., Seth, R., Knott, P.D., et al. (2015). Human satellite cell transplantation and regeneration from diverse skeletal muscles. Stem Cell Reports *5*, 419–434.

Yu, J., Vodyanik, M.A., Smuga-Otto, K., Antosiewicz-Bourget, J., Frane, J.L., Tian, S., Nie, J., Jonsdottir, G.A., Ruotti, V., Stewart, R., et al. (2007). Induced pluripotent stem cell lines derived from human somatic cells. Science *318*, 1917–1920.

Stem Cell Reports, Volume *15*

Supplemental Information

Induced Fetal Human Muscle Stem Cells with High Therapeutic Potential in a Mouse Muscular Dystrophy Model

Mingming Zhao, Atsutoshi Tazumi, Satoru Takayama, Nana Takenaka-Ninagawa, Minas Nalbandian, Miki Nagai, Yumi Nakamura, Masanori Nakasa, Akira Watanabe, Makoto Ikeya, Akitsu Hotta, Yuta Ito, Takahiko Sato, and Hidetoshi Sakurai

Figure. S1

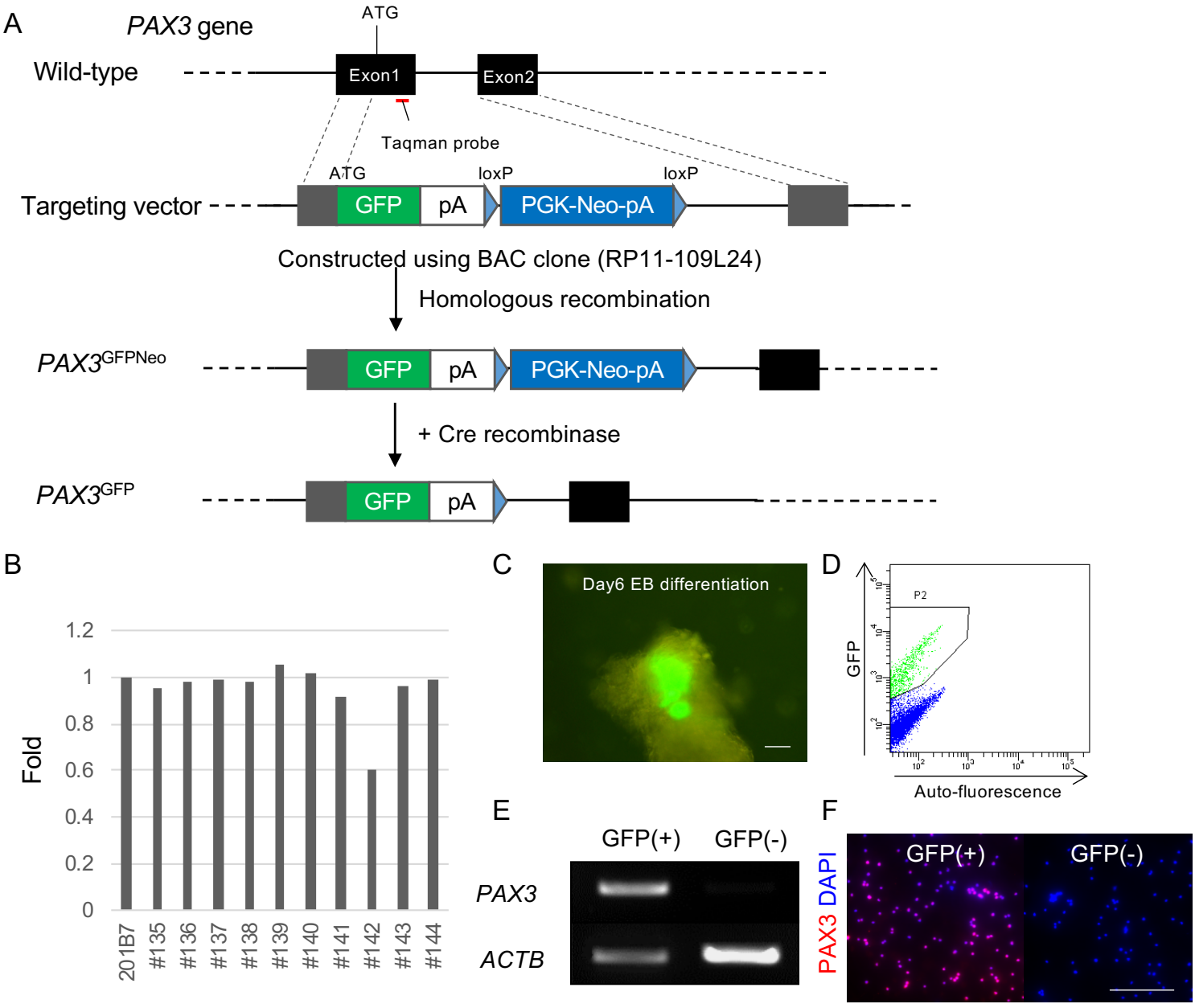

Supplemental Fig S1. Generation of PAX3-GFP Knock-in (KI) hiPSC line (201B7). Related to Figure1.

(A) Schematic picture demonstrates homologous recombination (HR) using BAC-based vectors to generate the PAX3 GFP knock-in hiPSC line. Knock-in cells were selected by G418, and the monoclonal cell population was isolated. The loxP-Neo-loxP cassette was removed by Cre recombinase. (B) Genotyping using RT-PCR with Taqman probe hybridizing at exon1 in the *PAX3* gene. The results show #142 is heterozygous. (C) Fluorescence micrographs of hiPSC-derived EBs that expressed PAX3-GFP. Scale bar, 200 μm. (D) Representative flow cytometry plots showing GFP+ and GFP- populations. (E) Gene expression of *PAX3* in the GFP+ and GFP- populations was analyzed by RT-PCR. (F) Immunocytochemistry shows PAX3 expression in GFP+ and GFP- cells after single cell plating.

Figure. S2

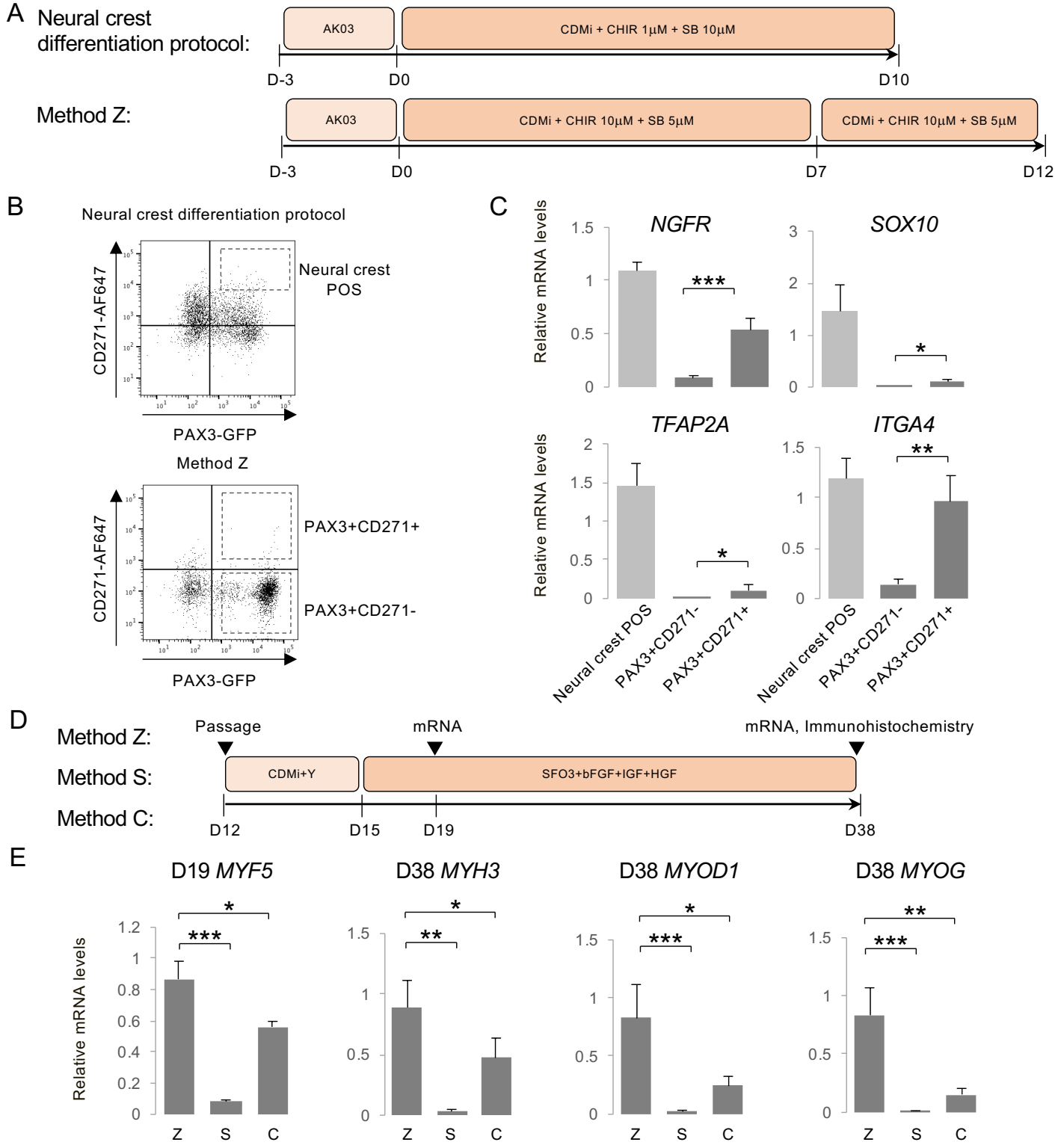

Supplemental Fig S2. Detecting neural crest marker expression in PAX3+/CD271- and PAX3+/CD271+ populations. Related to Figure 2.

(A) Timeline of hiPSCs to neural crest lineage using a neural crest differentiation protocol (Fukuta et al., 2014) and timeline of hiPSCs to dermomyotome differentiation using method Z (Zhao et al. this work). (B) FACS sorting of PAX3+/CD271+ at day 10 (D10) differentiation in the neural crest differentiation protocol. FACS sorting of PAX3+/CD271- and PAX3+/CD271+ population at day 12 (D12) of differentiation in method Z. (C) The neural crest marker gene expression in PAX3+/CD271- and PAX3+/CD271+ cells in method Z. The PAX3+/CD271+ population in the neural crest differentiation protocol was a positive control (Neural crest POS). Data of three independent experiment are shown as means ± S.D., *$p < 0.05$, **$p < 0.01$, ***$p < 0.001$. (D) After 12 days of differentiation in method Z, method S, or method C, the cells were passaged on Matrigel-coated plates at the same cell density and stimulated with myogenic differentiation medium. (E) The myogenesis marker gene expression in method Z, method S and method C. Data of three independent experiment are shown as means ± S.D., *$p < 0.05$, **$p < 0.01$, ***$p < 0.001$.

Figure. S3

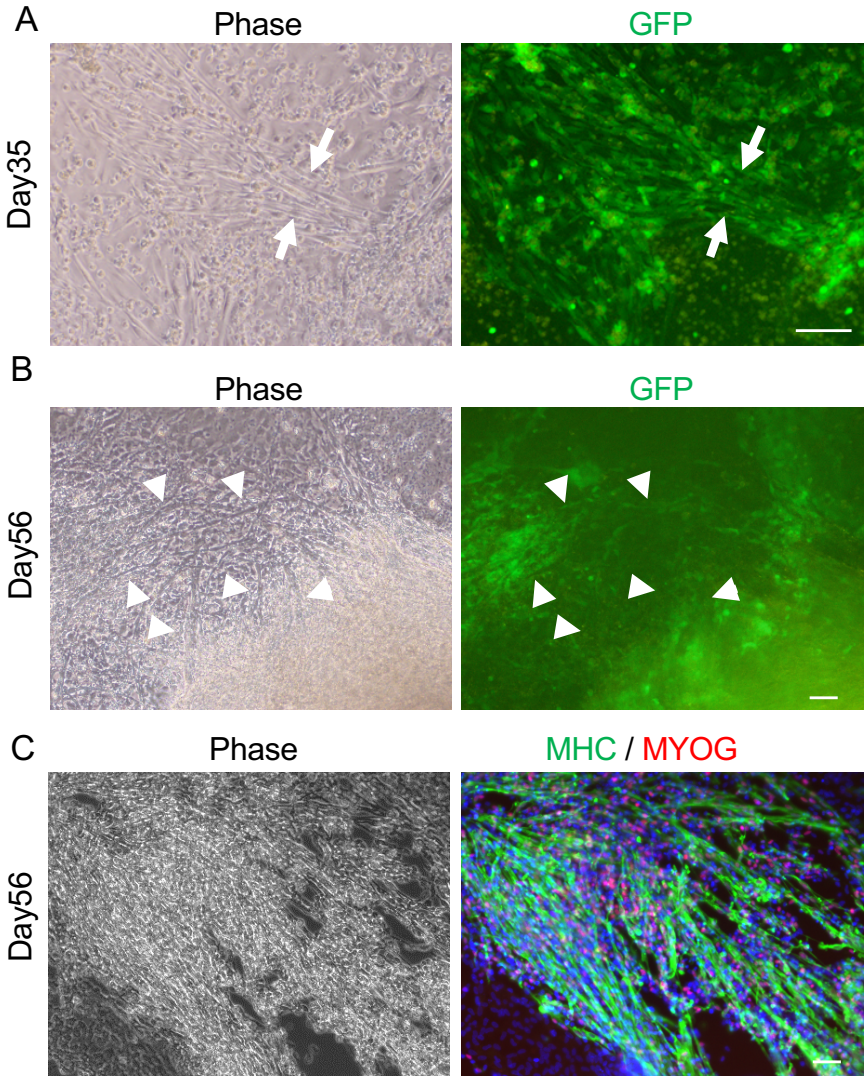

Supplemental Fig S3. Myogenic differentiation of the PAX3-GFP KI cell line. Related to Figure 1.
(A) Phase and fluorescence micrographs of hiPSCs differentiated for 35 days. Arrows, differentiated myofibers with GFP+ cells. Scale bar, 100 μm. (B) Phase and fluorescence micrographs of hiPSCs differentiated for 56 days. Arrowheads, differentiated myofibers without GFP+ cells. Scale bar, 100 μm. (C) Phase and fluorescence micrographs of hiPSCs differentiated for 56 days. Immunohistochemistry with myosin heavy chain (MHC) (Green) and MYOGENIN (MYOG) (Red) antibodies. Scale bar, 100 μm.

Figure. S4

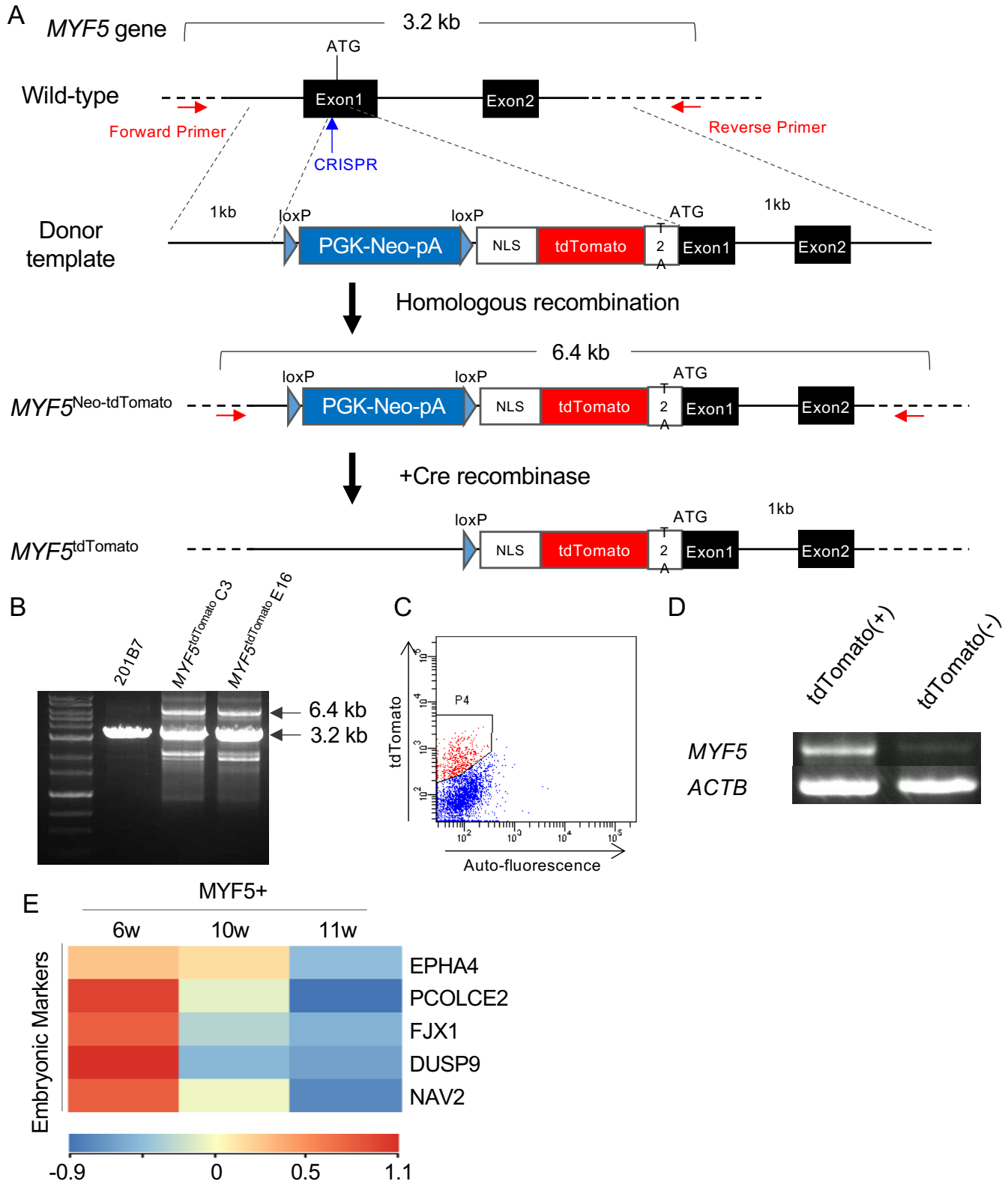

Supplemental Fig S4. Generation of MYF5-tdTomato KI hiPSC line (201B7). Related to Figure 3 & 4.
(A) Schematic overview depicting the MYF5-tdTomato cell line establishment strategy. Top line shows the *MYF5* gene structure. The blue arrow indicates the CRISPR cut site, and the red arrows indicate the forward and reverse primers for genotyping. The homologous arms of the donor vector are indicated as the left arm (1 kb) and right arm (1 kb). Knock-in cells were selected by G418, and the monoclonal cell population was isolated. The loxP-Neo-loxP cassette was removed by Cre recombinase. (B) PCR genotyping using the primers in (A) indicates C3 and E16 are heterozygous. PCR revealed the wild type band (3.2 kb) and Neo-tdTomato KI band (6.4 kb). (C) Representative flow cytometric plots showing the MYF5-tdTomato^{+} and MYF5-tdTomato^{-} populations. (D) RT-PCR analysis of the *MYF5* gene expression in the tdTomato+ and tdTomato- populations. (E) Heat map of embryonic marker gene expression in MYF5+ cells differentiated for 6, 10 or 11 weeks (green is low expression and red is high).

Figure. S5

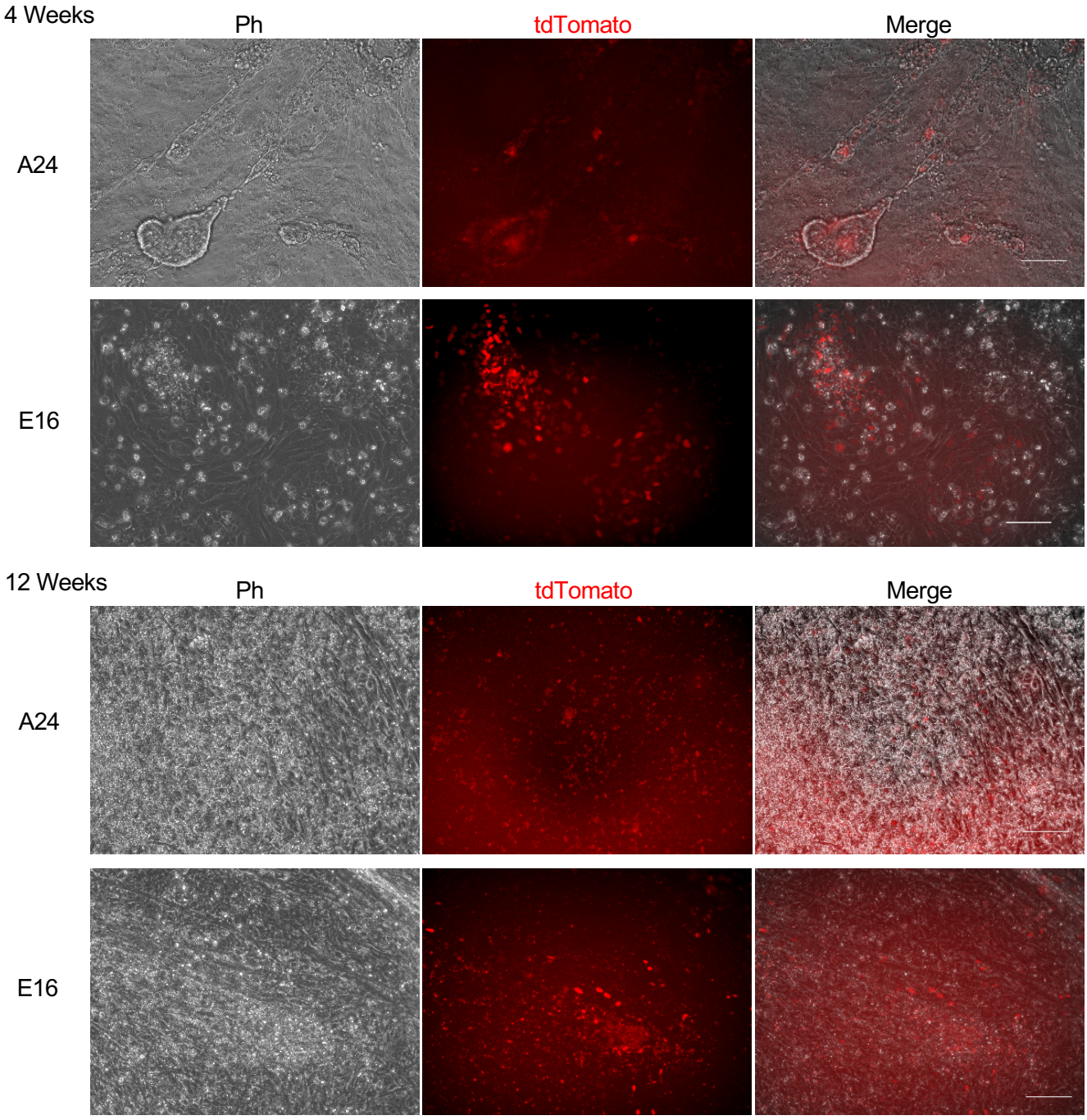

Supplemental Fig S5. Phase and fluorescence images of MYF5-tdTomato reporter cells. Related to Figure 3. Representative bright field (Phase, Ph), tdTomato and merged images of live cultures of MYF5-tdTomato cells at 4 weeks and 12 weeks in A24 and E16 cell lines. Scale bars = 50 µm.

Figure. S6

MYF5- at 12-weeks of differentiation

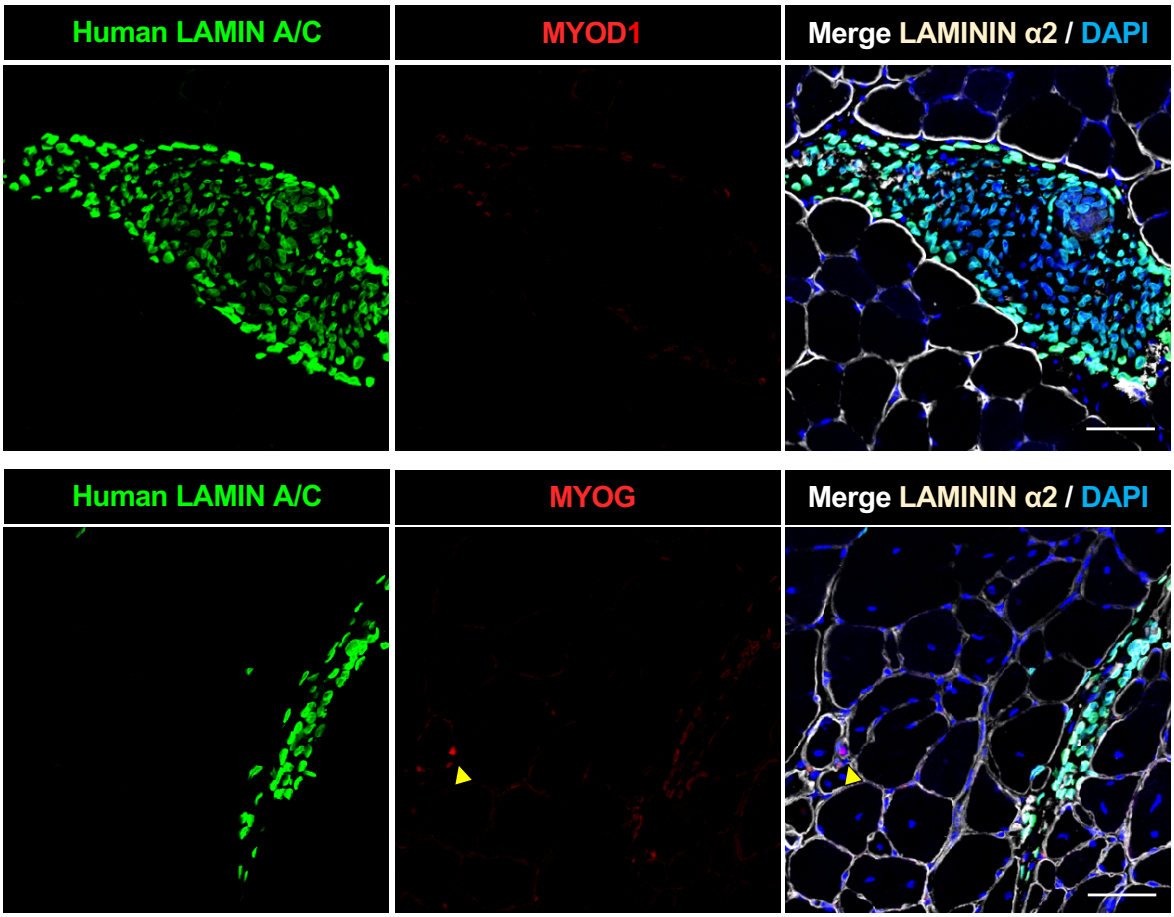

Supplemental Fig S6. Characterization of the engrafted cells derived from MYF5- cells. Related to Figure 5
12-weeks differentiated MYF5- cells were sorted and transplanted into the tibialis anterior muscles of Ctx treated NSG mice. The engrafted cells were evaluated by immunohistochemistry. Immunohistochemistry of human LAMIN A/C (green), MYOD1 (upper, red), MYOGENIN (MYOG) (lower, red), LAMININ α2 (white) and DAPI (blue) at 4 weeks after transplantation. Scale bars, 50 μm. Yellow arrowheads indicate murine myogenic cells. MYF5- cell-derived engrafted cells mainly consisted of non-myogenic cells.

Figure. S7

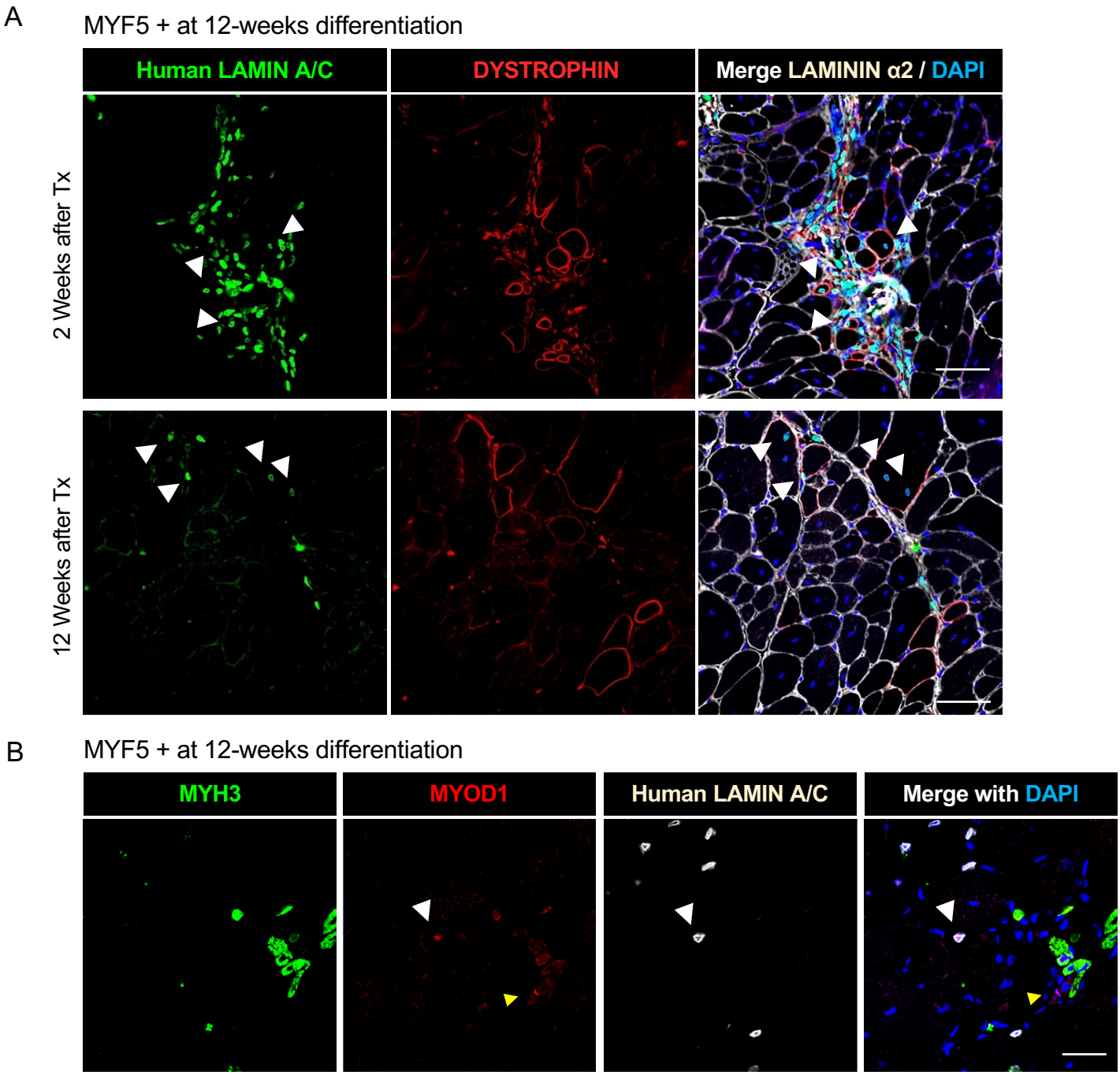

Supplemental Fig S7. Characteristics of the engrafted MYF5+ cells in DMD-null/NSG model mice. Related to Figure 6

(A) 12-weeks differentiated MYF5+ cells were sorted and transplanted into the tibialis anterior muscles of DMD-null/NSG model mice. The engrafted cells were evaluated by immunohistochemistry. Immunohistochemistry of human LAMIN A/C (green), DYSTROPHIN (red), LAMININ α2 (white) and DAPI (blue) at 2 (upper) or 12 (lower) weeks after transplantation. White arrows indicate DYSTROPHIN+ myofibers. White arrowheads indicate engrafted human cells. Scale bars, 50 μm. The size of the DYSTROPHIN+ myofibers at 2 weeks after treatment was smaller than normal mouse myofibers, but the same size at 12 weeks. (B) 12-weeks differentiated MYF+ cells were sorted and transplanted into the tibialis anterior muscles of DMD-null/NSG model mice. The engrafted cells were evaluated by immunohistochemistry. Immunohistochemistry of embryonic myosin heavy chain (MYH3, green), MYOD1 (red), human LAMIN A/C (white) and DAPI (blue) at 4 weeks after transplantation. White arrows indicate DYSTROPHIN+ myofibers. White arrowheads indicate human cell-derived MYOD1 positive cell. Yellow arrowheads indicate murine MYOD1 positive cell. Scale bars, 50 μm.

References

Fukuta, M., Nakai, Y., Kirino, K., Nakagawa, M., Sekiguchi, K., Nagata, S., Matsumoto, Y., Yamamoto, T., Umeda, K., Heike, T.*, et al.* (2014). Derivation of mesenchymal stromal cells from pluripotent stem cells through a neural crest lineage using small molecule compounds with defined media. PLoS One *9*, e112291.

Supplemental Table 1. qRT-PCR Primer Sets

Gene	Forward Sequence	Reverse Sequence
T	ACCCAGTTCATAGCGGTGAC	CATTGGGAGTACCCAGGTTG
TBX6	AGCCTGTGTCTTTCCATCGT	AGGCTGTCACGGAGATGAAT
PAX3	AGGAAGGAGGCAGAGGAAAG	CAGCTGTTCTGCTGTGAAGG
MEOX1	GAGATTGCGGTAAACCTGGA	GAACTTGGAGAGGCTGTGGA
SIX1	AGTTCTCGCCTCACAACCAC	ACACCCCTCGACTTCTCCTT
MYF5	TCACCTCCTCAGAGCAACCT	GGAACTAGAAGCCCCTGGAG
PAX7	AGGGCCTCCTGCTTGTTTAT	GGTTTTGCCCAACTCAGTGT
MYOD1	ACGTGAGGACGAGCATGTG	GTGCAGCGCTTGAGTGTCT
MYOGENIN(MYOG)	TGGGCGTGTAAGGTGTGTAA	CGATGTACTGGATGGCACTG
NFIX	CTGGAGTCAGACCAGGGAGC	GGGCTCGACTGCTGGATGAT
COL15A1	CGTGTTAGAGATGGCTGGA	GTTTGGTGGAGGCAGAAG
CD44	CCAGAAGGAACAGTGGTTTGGC	ACTGTCCTCTGGGCTTGGTGTT
CRYAB	CTTTGACCAGTTCTTCGGAG	CCTCAATCACATCTCCCAAC
DLK1	AAGGACTGCCAGAAAAAGGAC	GCAGAAATTGCCTGAGAAGC
RPLP0	AAACGAGTCCTGGCCTTGTCT	GCAGATGGATCAGCCAAGAAG
NOGGIN	CCTCATCGAACACCCAGACC	CATGAAGCCTGGGTCGTAGTG
PARAXIS	TCCTGGAGAGCTGTGAGGAT	CACACCCTGTCACCAACAGT
DMRT2	GAACCACCAAGCAAGGACTTC	CCCAGACCCTGAATACTGCAT
ALX4	TCCACTGCATATGAGCTGC	GTTGTTGCCGAGCCAGGA
EN1	GACTCGGACAGGTGCTATCG	AGTTCGCAGTTTCGTCCCTT
MYH3	GCAGATTGAGCTGGAAAAGG	TCAGCTGCTCGATCTCTTCA
SOX10	CGGACCAGTACCCGCACCT	GGCGCTTGTCACTTTCGTTCA
TFAP2A	AAGAGTTCACCGACCTGCTG	AGGGCCTCGGTGAGATAGTT
NGFR	CAGGCTTTGCAGCACTCAC	CTGCTGCTGTTGCTGCTTCT
ITGA4	GCTTCTCAGATCTGCTCGTG	GTCACTTCCAACGAGGTTTG

Supplemental Table 2. Primers Lists and Template Genes for Construction of Plasmids

Part of Fragment		Sequence
For Reporter Plasmids		
MYF5-5' Arm	Fw	CGGTATCGATAAGCTCTCCCCAACCCAAATAACC
	Rv	GCTATACGAAGTTATATAAAGAACCCCAACCCCAG
	Template	Human Genome
LoxP-Neo-pA-LoxP	Fw	TGGAGCCATGGTGGCATAACTTCGTATAATGTATGCTATACGAAGTTATCAATTGTCTAGACAATTGGC
	Rv	GCTATACGAAGTTATATAAAGAACCCCAACCCCAG
	Template	pBS-FloxedNeo
NLS-tdTomato T2A	Fw	GCCACCATGGCTCCAAAA
	Rv	TGGGCCGGGATTCTCCTCCACGTCGCCGCATGTCAGCAGGCTTCCTCTGCCCTCCTTGTACAGCTCGTCCATGC
	Template	pCMV-NLS-tdTomato
MYF5-ATG-Exon1	Fw	GAGAATCCCGGCCCAATGGACGTGATGGATGGC
	Rv	AGCTGGAGCTCCACCCTGACCAAAGGTGAGGCTGT
	Template	Human Genome
For sgRNA Plasmids		
MYF5 sgRNA	Fw	GAGACCACTTGGATCCGATCCCTCTCGCTGCCGTCCGTTTTAGAGCTAGAAATAGCA
	Rv	GCCCGGGTTTGAATTCAAAAAAAGCACCGACTCGGTGCCACTTTTTCAAGTTGATAACGGACTAGCCTTATTTTAACTTGCTATTTCTAGCTC
	Template	-

Supplemental Table 3. Primers Lists for Validation of Reporter Line.

Use		Sequence
For Integration Check	Fw1	TGAACTGGGTTACCCTAGATTGAGTTGAG
	Rv1	AGGCCAGAGGCCACTTGTGTAGC
	Fw2	ATGCGGCGACGTGGAGGAGAATC
	Rv2	ACCCAGAGGTCAGGTGGTCACAG
For Copy Number Check	Fw	CCTGAATGAACTGCAGGACG
	Rv	CTTCCCGCTTCAGTGACAAC
For Sequencing	Fw1	TGAACTGGGTTACCCTAGATTGAG
	Fw2	AGGACAACAACATGGCCGTCATC
	Fw3	ATGCGGCGACGTGGAGGAGAATC
	Fw4	CCTGAATGAACTGCAGGACG
	Rv1	ACCCAGAGGTCAGGTGGTCACAG
	Rv2	AGGCCAGAGGCCACTTGTGTAGC
	Rv3	CCTAAACTGGGTACATGAGAATGG
	Rv4	CTTCCCGCTTCAGTGACAAC

Supplemental Table 4. Antibody list and dilution ratio

1st Antibody	Source	Clonarity	Dilution	Company
CD271-AF647	mouse mono	IgG1	1:20	BD Pharmingen
Myoshin Heavy chain (MHC) MF20	mouse mono	IgG2b	1:800	eBioscience
MYOGENIN (MYOG) F5D	mouse mono	IgG1	1:500	Santacruz
PAX7	mouse mono	IgG1	1:100	DSHB
MYOD1	rabbit mono	IgG	1:500	Abcam
Human SPECTRIN	mouse mono	IgG2b	1:200	Leica
Human Nuclei	mouse mono	IgG1	1:200	Millipore
LAMININ α2	rat mono	IgG	1:150	ALEXIS
DYSTROPHIN	rabbit poly	IgG	1:1000	Abcam
Human LAMIN A/C	mouse mono	IgG2b	1:200	Leica
eMyHC (MYH3)	rabbit poly	IgG	1:400	Sigma
PAX3	rabbit poly	IgG	1:100	Gene Tex
2nd Antibody			Dilution	Company
Alexa Fluor 568 conjugated goat-anti-mouse IgG2b			1:500	Invitrogen
Alexa Fluor 488 conjugated goat-anti-mouse IgG1			1:500	Invitrogen
Alexa Fluor 568 conjugated goat-anti-mouse IgG1			1:500	Invitrogen
Alexa Fluor 488 conjugated goat-anti-rabbit IgG			1:500	Invitrogen
Alexa Fluor 488 conjugated goat-anti-mouse IgG2b			1:500	Invitrogen
Alexa Fluor 647 conjugated goat-anti-rat IgG			1:500	Invitrogen
Alexa Fluor 568 conjugated goat-anti-rabbit IgG			1:500	Invitrogen

Supplemental Experimental Procedures

Human iPSC lines and maintenance culture

HiPSC clone 201B7(Takahashi et al., 2007) was used as the parental cell line for generating the PAX3-GFP and MYF5-tdTomato reporter lines. All hiPSCs were cultured and maintained in feeder-free culture on iMatrix-511 (Nippi) in StemFit AK02N medium (Ajinomoto) as previously described(Nakagawa et al., 2014).

RNA extraction and quantitative real-time RT-PCR (qRT-PCR)

Total RNA was extracted with the ReliaPrep RNA Cell Miniprep system (Promega, Z6012). cDNA synthesis was carried out with the ReverTra Ace qPCR RT kit (TOYOBO, FSQ-101). qRT-PCR was carried out with the SYBR Green system (Applied Biosystems) and a One Step thermal cycler (Applied Biosystems) and was performed in triplicate for each sample. *Beta-actin* or *RPLP0* was used as the internal control. Primer sets used in this study are listed in Supplemental Table S1.

Generation of PAX3-GFP reporter cell line

The human BAC clone RP11-109L24 was purchased from Invitrogen. The construction and recombination of the targeting vector were performed as described(Mae et al., 2013). The primers used for the construction were as follows: hPAX3-EGFP-S, 5'-TAATTTCCGAGCGAAGCTGCCCCCAGGATGACCACGCTGGCCGGCGCTGTGCCCAGGATGATGGTGAGCAAGGGCGAGG-3'; and hPAX3-PN-AS, 5'-GGGTGAGGCAGCCGGTCCCAGGCCCTGGGATCCAGGCGGCGCGCTGAGGCCCTCCCTTACGTCGACGGCGAGCTCAGACG-3'. Electroporation of the BAC construct into 201B7 was carried out as previously described(Mae et al., 2013). The gene targeted clone was selected by the Taqman PCR assay. RT-PCR reactions were carried out with 100 ng of genomic DNA, 250 nM of Taqman probes and 500 nM of primers. The sequences of the primers were as follows: PAX3 Fw, 5'-GGATATATTTCCGAGCGAAGCT-3'; PAX3 Rv, 5'-GGCCCTCCCTTACCTTCCA-3'; and PAX3 probe, 5'-(FAM)-ACGCGGGTAGTTCT-3'. We selected clone #142, which showed approximately half the expression level of the targeted site, as a heterozygous targeted PAX3-GFP knocked-in clone. To remove the PGK-Neo cassette, 2 μg Cre expression vector pcDNA3-nVenus-Cre was transfected into the targeted 201B7 cells by the FuGENE HD lipofection system (Roche). After the isolation of 24 clones, removal of the PGK-Neo cassette was confirmed by adding G418 (Nacalai tesque) in a separately prepared culture well.

Generation of MYF5-tdTomato reporter cell line

To construct the donor template vector for td-Tomato knock-in of the *MYF5* gene, the following four fragments, *MYF5*-5'-UTR, LoxP-Neo-pA-LoxP, tdTomato-P2A and *MYF5*-Exon1, were integrated into the HindⅢ-Sac Ⅰ site of the pBS Ⅱ SK(+) vector by the In-Fusion HD Cloning kit (Clontech). Each fragment was cloned by PCR (KOD Plus Neo, TOYOBO). All primers used in the PCR are listed in Supplemental Table 2. Before the transfection experiments, plasmid DNAs were purified by the NucleoBond Xtra Maxi Plasmid DNA Purification kit (Macherey-Nagel).

To construct the sgRNA expression vector, two oligos containing the sgRNA target site and a universal reverse primer were PCR amplified and cloned into the BamHI-EcoRI site of the pHL-H1-ccdB-mEF1α-RiH vector. All primers are listed in Supplemental Table 2.

Together with the Cas9 expression vector, the donor template vector and the sgRNA expression vector were electroporated into 201B7 iPSCs as previously described(Li et al., 2015). Briefly, transfection was performed with a NEPA 21 Electroporator (Nepagene) as follows. The poring pulse was set to pulse voltage, 125 V; pulse width, 5 ms; pulse number, 2. HiPSCs were pretreated with a ROCK inhibitor (10 μM Y-27632; Sigma) for at least 1 hr before electroporation and dissociated into single cells with 0.25% Trypsin solution treatment for 5 min at 37℃. 1.6 μg of Cas9 plasmid, 0.5 μg of sgRNA plasmid and 2.5 μg of reporter plasmid were electroporated into $1x10^6$ cells. After electroporation, the cells were plated onto an iMatrix-511-coated 10 cm dish in the presence of 10 μM Y-27632 for 2 days.

48 hr after the electroporation, the hiPSCs were treated with 100 μg/ml G418 for the selection of transfected cells. After subcloning the 24 colonies, genome DNA was extracted from each clone for genotyping. To establish reporter lines with heterozygous td-Tomato knocked-in, genomic PCR was done with Fw1-Rv1 primer pairs (Supplemental Table 3), and copy numbers of the knocked-in construct were checked by qRT-PCR with Fw-Rv primer pairs (Supplemental Table 3). The sequences of these clones were checked with the primers listed in Supplemental Table 3. After confirmation, two clones were selected and then transfected with 5 μg CRE expression vector pCMV-Cre-puro to remove the LoxP-Neo-pA-LoxP cassette. After transfection, we picked up several clones and sequenced each genome in order to confirm the construction was correctly knocked-in. Two heterozygous clones (C3 and E16) and one homozygous clone (A24) were selected for the subsequent experiments.

Myogenic differentiation

HiPSCs were dissociated with Accutase (Nacalai) and plated as single cells on a Matrigel-coated 6-well plate (10,000 cells/well) in Stemfit (AK02N, Ajinomoto) supplemented with ROCK inhibitor (10 μM, Y-

27632, Sigma) for 2 days. The medium was changed to fresh Stemfit, in which the cells were kept for one day. Afterwards, the medium was changed to differentiation medium, which contained CDMi supplemented with CHIR99021 (CHIR, Axon MedChem, Tocris) and SB431542 (SB, Sigma). CDMi contains IMDM (+) L-Glutamine (+) 25 mM HEPES (Invitrogen, 12440053) and F12 (1X) Nutrient Mixture (Ham) (+) L-Glutamine (Invitrogen, 11765054) at the ratio 1:1 supplemented with 1% BSA (Sigma), 1% Penicillin-Streptomycin Mixed Solution (Nacalai), 1% CD Lipid Concentrate (Invitrogen), 1% Insulin-Transferrin-Selenium (Invitrogen) and 450 µM 1-Thioglycerol (Sigma). After 7 days of differentiation, the cells were dissociated with Accutase (Nacalai) and plated as single cells on a Matrigel-coated 6-well plate (400,000 cells/well) in CDM supplemented with CHIR, SB and a ROCK inhibitor (10 µM Y-27632, Sigma). At differentiation day 14, the cells were dissociated with Accutase (Nacalai) and plated as single cells on a Matrigel-coated 6-well plate (400,000 cells/well) in CDM supplemented with Y-27632. The medium was changed to serum-free culture medium (SF-O3; Sanko Junyaku) supplemented with 0.2% bovine serum albumin (BSA), 0.1 mM 2-mercaptoethanol (2-ME), 10 ng/ml recombinant human IGF-1 (PeproTech), 10 ng/ml recombinant human bFGF (Oriental Yeast CO., LTD, NIB 47079000) and 10 ng/ml recombinant human HGF (PeproTech). The medium was then changed every 2 or 3 days from day 17 to day 38. Finally, the medium was changed to DMEM (Invitrogen, 11960069) supplemented with 0.5% Penicillin-Streptomycin (Nacalai, 26253-84), 2 mM L-glutamine (Nacalai, 16948-04), 0.1 mM 2-ME, 2% Horse Serum (HS, Sigma), 5 µM SB and 10 ng/ml IGF-1 (Peprotech) until week 12. In figure 2, the cells were differentiated to dermomyotome-like cells following the protocol of Method S (Shelton et al., 2014) or Method C (Chal et al., 2015).

Cell preparation for FACS analysis

Cells after 6 weeks of differentiation were treated with collagenase-1 for 30-60 min at 37℃ and neutralized with DMEM +2% HS. Then the cells were centrifuged at 1000 rpm, 4℃ for 10 min. Cells before 6-weeks differentiation did not undergo this collagenase treatment. After removal of the supernatant, the cells were treated with Accutase at 37℃ for 5 min and neutralized with DMEM +2% HS. Then the cells were centrifuged at 1000 rpm, 4℃ for 10 min. After removal of the supernatant, the cells were suspended with HBSS buffer containing 1% Hoechst and filtered with a 40 µm mesh. The prepared cells were stocked on ice before the FACS analysis.

FACS Analysis

Analysis. FACS analysis was performed by using an AriaII (BD) according to the manufacturer's protocol. 1 x 10^6 PAX3-GFP cells in a 100 µl experimental sample were stained with 5 µl CD271-AF647

antibody (BD, 560326) for 20 min on ice. Gating was determined for the PAX3-GFP cell line using hiPSCs and undifferentiated culture as the baseline control.

Sorting. MYF5+ cells were isolated by FACS at 6, 10, 11, or 12 weeks of differentiation. Sorted populations were either processed for qRT-PCR or for the transplantation experiments.

Re-culture Protocol

Sorted cells were centrifuged at 4℃ for 30 min. After removal of the supernatant, the cells were suspended in the maturation medium with 10 μM Y-27632. Then the cells were plated onto a 6-well collagen type 1-coated plate at 1-3x10^5 cells/well.

Immunocytochemistry

Differentiated cell samples were directly fixed with 2% paraformaldehyde (PFA, Nacalai tesque) for 10 min at 4℃ in a culture dish. Alternatively, sorted cells were seeded onto glass slides with Smear Gel (GenoStaff) and fixed with 2% PFA for 10 min at 4℃. Then the cells were washed twice with PBS and blocked by Blocking One (Nacalai) for 30 min at 4°C. The cells were stained with the appropriate primary antibodies diluted in 10% Blocking One in PBS for 16 hr at 4°C. After three washings with 0.2% Triton X-100 (Sigma-Aldrich) in PBS (PBST), the cells were stained with the appropriate secondary antibodies for 1 hr at room temperature. DAPI, a nuclear stain (Sigma), was loaded at 1:5000 dilution for 5 min. All antibodies are listed in Supplemental Table 4. The samples were observed by using a BZ-X700 (Keyence, Osaka, Japan), and the MHC-positive area was measured by using BZ-X analyzer software (Keyence, Osaka, Japan).

Immunohistochemistry

Engrafted muscles were frozen in isopentane (Wako) cooled in liquid nitrogen. Serial 10 μm cryosections were collected. Tissue sections or cells were fixed in 4% PFA for 20 min at room temperature and washed twice with PBS for 5 min at room temperature. After blocking with Blocking One for 1 hr at room temperature, the tissue samples were incubated with primary antibodies diluted in Can Get Signal B solution (TOYOBO) for 16 hr at 4°C. After washing with PBST three times, the samples were stained with the appropriate secondary antibodies diluted in Can Get Signal B solution for 1 hr at room temperature. The immunostained samples were mounted in VECTA SHIELD mounting medium with DAPI (Vector Laboratories). To measure the localization of the engrafted cells, human LAMIN A/C positive nuclei were counted in the entire area of six TA sections per one transplanted tissue co-stained with DYSTROPHIN and

LAMININ α2. A total of four transplanted tissues were analyzed. The samples were observed by using a LSM700 confocal microscope (Carl Zeiss, Oberkochen, Germany). The primary and secondary antibodies are listed in Supplemental Table 4.

Microarrays analysis

Total RNA was isolated using the ReliaPrep^{TM} RNA Miniprep System (Z6012). The sequencing libraries were constructed using the TruSeq Stranded mRNA Library Prep Kit (Illumina) and sequenced in 100 cycle Single-Read mode of HiSeq2500. All sequenced reads were extracted in FASTQ format using BCL2FASTQ Conversion Software 1.8.4 in the CASAVA 1.8.2 pipeline. FASTQ converted reads were mapped to hg19 reference genes using TopHat v2.0.8b and quantified using RPKMforgenes. The analyses were performed using R ver. 3.1.0. Heat maps of embryonic and fetal muscle progenitor marker expression were generated by Genespring GX 13 software.

Muscle contraction assay

1-2 million MYF5-tdTomato positive cells were transplanted into the right gastrocnemius of DMD-null/NSG mice. The left gastrocnemius was used as the shammed control. Living mice were anesthetized by isoflurane (AbbVie). The maximum muscle contraction force of both sides of the gastrocnemius was analyzed at 2, 4 and 6 weeks after the transplantation with the custom-made mouse ankle joint motor function analysis system (Bio Research Center) previously described(Itoh et al., 2017).

Supplemental References

Chal, J., Oginuma, M., Al Tanoury, Z., Gobert, B., Sumara, O., Hick, A., Bousson, F., Zidouni, Y., Mursch, C., Moncuquet, P.*, et al.* (2015). Differentiation of pluripotent stem cells to muscle fiber to model Duchenne muscular dystrophy. Nat Biotechnol *33*, 962-969.

Itoh, Y., Murakami, T., Mori, T., Agata, N., Kimura, N., Inoue-Miyazu, M., Hayakawa, K., Hirano, T., Sokabe, M., and Kawakami, K. (2017). Training at non-damaging intensities facilitates recovery from muscle atrophy. Muscle Nerve *55*, 243-253.

Li, H.L., Fujimoto, N., Sasakawa, N., Shirai, S., Ohkame, T., Sakuma, T., Tanaka, M., Amano, N., Watanabe, A., Sakurai, H.*, et al.* (2015). Precise correction of the dystrophin gene in duchenne muscular dystrophy patient induced pluripotent stem cells by TALEN and CRISPR-Cas9. Stem Cell Reports *4*, 143-154.

Mae, S.I., Shono, A., Shiota, F., Yasuno, T., Kajiwara, M., Gotoda-Nishimura, N., Arai, S., Sato-Otubo, A., Toyoda, T., Takahashi, K.*, et al.* (2013). Monitoring and robust induction of nephrogenic intermediate mesoderm from human pluripotent stem cells. Nat Commun *4*, 1367.

Nakagawa, M., Taniguchi, Y., Senda, S., Takizawa, N., Ichisaka, T., Asano, K., Morizane, A., Doi, D., Takahashi, J., Nishizawa, M*., et al.* (2014). A novel efficient feeder-free culture system for the derivation of human induced pluripotent stem cells. Sci Rep *4*, 3594.

Shelton, M., Metz, J., Liu, J., Carpenedo, R.L., Demers, S.P., Stanford, W.L., and Skerjanc, I.S. (2014). Derivation and expansion of PAX7-positive muscle progenitors from human and mouse embryonic stem cells. Stem Cell Reports *3*, 516-529.

Takahashi, K., Tanabe, K., Ohnuki, M., Narita, M., Ichisaka, T., Tomoda, K., and Yamanaka, S. (2007). Induction of pluripotent stem cells from adult human fibroblasts by defined factors. Cell *131*, 861-872.